

University of Memphis

University of Memphis Digital Commons

Electronic Theses and Dissertations

7-22-2010

Design and Evaluation of Chitosan-Calcium Phosphate Scaffolds Constructed from Air Dried and Lyophilized Microspheres

Duong T. Nguyen

Follow this and additional works at: <https://digitalcommons.memphis.edu/etd>

Recommended Citation

Nguyen, Duong T., "Design and Evaluation of Chitosan-Calcium Phosphate Scaffolds Constructed from Air Dried and Lyophilized Microspheres" (2010). *Electronic Theses and Dissertations*. 62.
<https://digitalcommons.memphis.edu/etd/62>

This Thesis is brought to you for free and open access by University of Memphis Digital Commons. It has been accepted for inclusion in Electronic Theses and Dissertations by an authorized administrator of University of Memphis Digital Commons. For more information, please contact khhgerty@memphis.edu.

To the University Council:

The Thesis Committee for Duong Thuy Nguyen certifies that this is the final approved version of the following electronic thesis: “Design and Evaluation of Chitosan-Calcium Phosphate Scaffolds Constructed from Air-dried and Lyophilized Microspheres.”

Joel D. Bumgardner, Ph.D.
Major Professor

We have read this thesis and
recommend its acceptance:

Warren O. Haggard, Ph.D.

Richard A. Smith, Ph.D.

Accepted for the Council:

Karen D. Weddle-West, Ph.D.
Vice Provost for Graduate Programs

DESIGN AND EVALUATION OF CHITOSAN-CALCIUM PHOSPHATE
SCAFFOLDS CONSTRUCTED FROM AIR DRIED AND LYOPHILIZED
MICROSPHERES

by

Duong Thuy Nguyen

A Thesis

Submitted in Partial Fulfillment of the

Requirements for the Degree of

Master of Science

Major: Biomedical Engineering

The University of Memphis

August 2010

ACKNOWLEDGEMENTS

I would like to acknowledge my research advisor and mentor, Dr. Joel D. Bumgardner, for his advice and directions through the beginning of my research career. His encouragements motivated me to be persistent and dedicated in my schoolwork and lab work.

I would like to thank my committee members – Dr. Warren O. Haggard and Dr. Richard Smith– for their guidance and expertise.

A special thanks to the biomedical engineering department at the University of Memphis and University of Tennessee Health Science Center. My fellow lab mates and colleagues – Marvin Mecwan, Andrew Noblett, Heather Doty, Drew Norowski, Jonathan McCanless, Megan Leedy, Monica Zugravu, and Egleide Elenes – for their insight and humor.

Most importantly my family, especially my mom, for their care and love.

ABSTRACT

Nguyen, Duong Thuy. MS. The University of Memphis. August/2010. Design and Evaluation of Chitosan-Calcium Phosphate Scaffolds Constructed from Air Dried and Lyophilized Microspheres. Major professor: Joel D. Bumgardner

The orthopedic clinical demand for bone grafts is a persistent problem for patients with age-related bone fractures and diseased bone defects. The aim of this study was to use calcium phosphate, a biomimetic ceramic with high compressive strength, and chitosan, a natural biodegradable and biocompatible polymer, to construct microsphere-based composite scaffolds to serve as a bone graft. Two types of scaffolds, (1) air-dried microspheres (AD) and (2) solid air-dried and lyophilized microsphere combination (FDAD), were evaluated *in vitro* for mineralization and enzymatic degradation. The combination FDAD scaffold showed on average ~80% increase ($p < 0.01$) in cell number per scaffold mass compared to AD because of the larger surface area advantage. Due to the higher cell number, the production of collagen was ~31% greater ($p < 0.01$) on FDAD scaffolds compared to AD scaffolds. However, scanning electron micrographs indicated minimal matrix deposition for both scaffold types. The AD scaffolds had a three-fold compressive strength advantage compared to FDAD scaffolds. These results indicate FDAD scaffolds have more osteogenic potential based on cell growth and collagen elaboration, but AD scaffolds demonstrated higher compressive strength.

PREFACE

This thesis presents research work on the construction and organization of composite chitosan calcium phosphate microsphere based scaffolds for use in bone tissue engineering. It is planned to have the results of this thesis work submitted as a manuscript to Journal of Biomedical Materials Research A.

TABLE OF CONTENTS

	Page
LIST OF FIGURES	vi
CHAPTER 1: Literature Review	1
Bone Biology	1
Bone Grafts	3
Bone Tissue Engineering	5
Summary	17
CHAPTER 2: Objectives and Significance	19
CHAPTER 3: Design and Evaluation of Chitosan-Calcium Phosphate Scaffolds Constructed from Air Dried and Lyophilized Microspheres	21
Abstract	22
Introduction	23
Methods and Materials	26
Results	32
Discussion	42
Conclusion	45
References	47
CHAPTER 4: Summary and Conclusions	50
CHAPTER 5: Future Works	53
References	55
Appendices	

LIST OF FIGURES

Figure 1. Images of AD and FDAD Scaffolds	31
Figure 2. Fluorescent Images of Scaffolds with Live/Dead®.....	32
Figure 3. SEM Images of AD and FDAD Scaffolds	33
Figure 4. DNA Normalized to Scaffold Mass.....	34
Figure 5. Alkaline Phosphatase Activity Normalized to DNA	35
Figure 6. Hydroxyproline Content Normalized to Scaffold Mass	36
Figure 7. Mass Change of AD and FDAD Scaffolds	37
Figure 8. Compressive Modulus of Degraded Scaffolds	38
Figure 9. FDAD Scaffold Before and After Compression	38

CHAPTER 1: LITERATURE REVIEW

Bone Biology

Bone is a complex and dynamic tissue in its physiological properties and three-dimensional (3D) organization. Bone responds to many physical, biological, and endocrine stimuli.¹ It is continually undergoing renewal depending on internal and external mediators. Bone tissue is considered a connective tissue with a complex organization consisting of bone cells embedded in bone extracellular matrix and bone marrow with its blood capillary network.^{2,3}

There are 206 bones in the adult body each providing structural support and rigid mechanical stability while allowing for flexibility with its variation in sizes, shapes, and joints.² In general, bone matrix is a composite of an organic matrix (collagen fibers and proteoglycans) and a mineral phase (hydroxyapatite-like) in which the ductile fibers reinforce the brittle hydroxyapatite minerals. This composite organization of bone provides high mechanical strength for protection against impact and trauma.¹⁻⁴

The architecture of bone can be classified into two types – cancellous and cortical – because of its density, porosity, and pore size. Cortical bone is the highly compact bone with 10% porosity and small pores while cancellous bone is 75-95% porous with pore sizes of 200-900 μm .² These differences dictate the mechanical strength and functionality each serve within the bone.^{2,3,5}

The highly dense cortical bone is found at the outer lining of most bones including long bone as the first line of defense against impact since it is stronger and heavier than cancellous bone. Its compressive modulus is about 17.0 GPa in the longitudinal direction, ~11.5 GPa in the transverse direction, and ~3.3GPa in shear.²

Cortical bone has a cylindrical organization of parallel collagen fiber layers called circumferential lamellae. Depending on the bone, there is a spatial difference between the outer and inner circumferential lamellae. These cylindrical lamellae are aligned longitudinal to the bone providing high compressive strength to transmit load. However, it is prone to fracture during perpendicular impact.²

Cancellous bone also known as trabecular or spongy bone is the interior network of struts or trabeculae in a 3D organization forming interconnections. Trabecular bone has the same lamellae organization but it is lighter and less stiff than cortical bone because of its porosity and orientation of the lamellae. The trabeculae are about 200µm in thickness for healthy bone with varying density but can reduce significantly with osteoporotic bone. The longitudinal compressive modulus for cancellous bone with long bones can vary according to location – 445MPa at the proximal tibia, 389MPa for the femur, and 291MPa for the lumbar spine.²

This dynamic tissue is continuously undergoing renewal regulated by osteogenic cells differentiated from mesenchymal stem cells (MSC), cytokines, and growth factors. Osteoblasts, osteoclasts, and osteocytes are the specialized bone cells responsible bone production, remodeling, and repair. During bone resorption and remodeling, osteoclasts are recruited to break down old bone while osteoblasts are recruited to synthesize new bone. When bone formation occurs, some osteoblasts are embedded within the matrix and differentiate into osteocytes. Osteocytes maintain bone viability and functionality by communicating with each other through small canals and with the rest of the body through the blood capillary system of bone marrow networking throughout bone.⁶ The

resorption process creates pits on the bone surface for the osteoblasts to settle to regenerate new bone at the eroded surface.⁶

When bone is injured, it has the inherent physiological response mechanisms to heal, repair, and remodel itself to its pre-injured condition. Bone fractures can vary in complexity and patterns. For small and simple fractures, the healing process can be initiated when the fracture site is stabilized allowing for biochemical and biomechanical stimulation of bone cells.⁶⁻⁸ The process starts with non-specific signaling to respond to the trauma causing inflammation and haematoma formation, proceeding to fracture bridging via soft callus, then hard callus formation, and finally specific regulation of bone remodeling.⁶⁻¹² Osteoclasts differentiated from MSCs remodel the woven hard callus into cortical and trabecular bone in the appropriate configuration.⁶ However, for more complex fractures and defects with critical size gaps (e.g. 8 mm in humans) that disrupt bone-to-bone interaction, normal physiological healing is inhibited, which will result in bone nonunion.¹³ Therefore, surgical intervention such as bone graft implantation in conjunction with internal fixation is required to restore the bone continuity and stability to induce bone union.

Bone grafts

In the United States alone, over 500,000 bone grafting procedures have been performed and demand will increase with age-related fractures as the ≥ 65 age group is projected to reach 51.5 million in 2020.^{14, 15} Implantation of bone grafts with internal fixation devices in long bone fractures promotes bone healing and formation to restore bone continuity at the fracture gap. The grafts serve as a temporary support with some

mechanical integrity and a favorable environment for osteogenesis, osteoconduction, and possible osteoinduction. Osteogenesis is the process of bone formation and regeneration.⁶ Osteoconduction is the facilitation of bone cell migration, differentiation, and mineralization while osteoinduction is an active facilitation of bone cell recruitment and formation by growth factors and cytokines embedded in the graft.⁶ Commonly used bone grafts are autografts and allografts which are extracted bone tissue that maintain some bone physiochemical properties.^{16, 17} However, there are limitations associated their use including prolonged surgical time and loss of bone bioactive properties.^{4, 18}

Autografts

The gold standard for treating large bone defects are autografts.¹⁸ Autografts are autologous bone commonly extracted from the iliac crest of the patient. The autograft retains its osteoinductive and osteoconductive properties but only some osteogenicity due to cell death during the transplanation.^{18, 19} However, the harvesting induces additional pain, blood loss, and surgical time to the patient, which can lead to tissue morbidity, healing delay, and other complications. For patients with old age or degenerative bone diseases, poor bone quality and other health risks, the use of autografts is limited. Also the quantity available for extraction is a limitation especially for patients with multiple fracture sites.⁵

Allografts

An alternative to autografts is allograft, which is donor bone tissue. The use of allografts accounts for more than one third of bone grafts used in the United States.⁵ Allografts are mostly used in a frozen irradiated or freeze-dried irradiated form. The

donor tissue undergoes controlled and regulated processes to remove the cellular phase and eliminate the possibility of immunological rejection along with viral transmission, respectively. However, these processes deteriorate the physiochemical and biomechanical properties of the donor bone by eliminating viable cells.^{1, 5, 20} For cancellous bone, there is no structural strength, no osteogenicity, and little osteoinductivity left after the harsh processing.²¹ For the cortical donor bone, there is no retention of osteoinductivity and osteogenicity.²¹ Furthermore, the variability in bone quality of the donor tissue is a major cause of variability in clinical results since responses are patient specific.⁵

Consequently, bone tissue engineering focuses the design and fabrication of synthetic constructs to serve as a bone graft substitute to overcome limitations of current auto- and allo-graft materials. Currently, there are commercially available synthetic bone scaffolds and substitutes for clinical applications including craniofacial defects, spinal fusion, and segmental bone loss.²²

Bone tissue engineering

In bone tissue engineering, researchers are investigating the potential to fabricate bone substitutes or scaffolds that can simulate physiological functions of bone for healing fractures and defects. The design criteria for constructing a scaffold are mimicry of bone's physical and biological properties. From the engineering perspective, an ideal scaffold is biocompatible, porous in structure for tissue infiltration and vascularization, osteoconductive, osteoinductive, biodegradable, and biomechanically strong to promote bone healing and regeneration.^{3, 16, 23} Furthermore, clinical needs require the scaffolds to have ease of handling, immediate functionality, retention of shape, and radiographically distinguishable.²⁴

a. Architecture

The shape and three-dimensional (3D) organization of the scaffold can affect the attachment, growth, and proliferation of bone cells, the exchange of nutrients and waste, and blood capillary formation.^{3, 16} Depending on the site of fracture, the 3D structure of the scaffold can vary from highly dense cortical bone to highly porous cancellous bone or a combination of both. For segmental bone repair like the femur, a combination of cortical and cancellous arrangement is necessary to mimic the functionality of the loss bone. Even though cortical bone is highly dense, it still has porosity. Porosity is an attribute of bone since bone is highly vascular to provide nutrition and communication exchange. Designs with interconnected pores >200µm have a continuous pathway that is more favorable for angiogenesis and cellular exchange of signaling and waste/nutrients.^{3, 23} However, high porosity can reduce the scaffold's mechanical strength so designs optimize between porosity and mechanical integrity.

In addition to overall architecture, surface micro-topography is also an important aspect for implant integration since surface roughness enhances attachment of cells and bone matrix.¹ Surface roughness can enhance osteoclast attachment and surface grooves guide osteoblast movements.^{25, 26}

b. Biocompatibility

The scaffolds should elicit no immune responses from the host that causes inflammation or rejection but instead promote responses to enhance bone healing and formation.¹⁶ The ideal scaffold environment promotes bone cell attachment, proliferation, and differentiation.¹ As the scaffold is resorbed, the by-products should be nontoxic and

easily excreted. Different synthetic and natural materials elicit by-products that are handled by the body in various ways.

c. Osteoinductivity

By functionalizing the scaffolds with growth factors and cytokines, the scaffold can induce mesenchymal stem cells to differentiate into osteoblasts to form new bone.²⁴ Inductive growth factors such as bone morphogenic proteins, vascular endothelial growth factors, and platelet-derived growth factors are currently used to up regulate bone cell morphogenesis and osteogenesis.²⁰ These factors are regulators at different phases of bone healing. For example, in phase 1 of healing, cells secrete a large variety of signaling molecules such as interleukins, fibroblast growth factors, and platelet derived growth factors (PDGF) for the recruitment of inflammatory cells, fibroblasts, and repair cells that initiate the other phases in bone healing.^{6, 12} Bone morphogenetic protein (BMP) and fibroblast growth factor are the major signaling molecules for ossification or remodeling soft callus into hard bone-like tissue.²⁷ Angiogenesis or the process of new blood vessel formation occurs in tandem to bone healing under the control of vascular endothelial growth factor (VEGF) and the angiopoietin pathway.⁹ Cytokines including macrophage-colony stimulating factor (M-CSF) (haematopoietic stem cell) and receptor activator of NF κ B ligand (RANKL) regulate the resorption and regeneration of osteoclast and osteoblasts.^{6, 20, 27}

d. Osteoconductivity

To enhance bone regeneration, the scaffold should stimulate bone cell differentiation, extracellular matrix deposition and mineralization. Natural ceramics

(calcium phosphate) and natural polymers (collagen fibers) are biomaterials native to bone that have characteristics to encourage the bone cell attachment and vascular infiltration.¹² Scaffolds made from ceramics can provide the minerals needed for bone cell mineralization. Furthermore, ceramic and collagen based scaffolds have good affinity for proteins like glycosaminoglycans (GAGs) found in the cell membrane and extracellular matrix.¹²

e. Biodegradability

The scaffold serves as a temporary support and template for bone regeneration at the defect site. Ideally, the scaffold is replaced by bone tissue during bone formation and regeneration through mechanisms that degrade or resorb the material.²⁸ Degradation can occur by different mechanisms such as hydrolysis, enzyme action, or a combination.²⁹ However, the rate of degradation should correlate to the rate of bone formation so that temporary structural support is replaced by the new bone tissue having load-bearing capacity.³⁰ The controllability of degradation is a goal for engineers to incorporate into the design of synthetic bone substitutes.

f. Biomechanical

Bone has range of mechanical properties (cortical modulus: ~17 GPa, cancellous modulus: 10-200 MPa), therefore, the scaffold must possess mechanical integrity similar to cancellous bone to prevent collapse of the scaffold used in conjunction with an internal device. The biomechanics of the scaffold correlates to the pore size, porosity, and rate of degradation. The balance between porosity, degradation, and strong biomechanics presents a challenge. At the initial time points of healing with little bone regeneration, the

scaffold strength should be equal or greater than that of the surrounding bone until new bone can bear the load. Currently, bone scaffolds are used in conjunction with internal fixation for fracture site stability to allow for good bone union and prevent collapse of graft tissue site. The internal fixation can assist the scaffold by transmitting most of the compressive load to encourage bone regeneration³. Scaffolds used in orthopedic applications especially in long bone fractures should possess compressive strength similar to that of cancellous bone (10-2000MPa).³¹

Biomaterials used in Tissue Engineering

Fabricating a bone scaffold to contain all these essential characteristics is a significant challenge for researchers to overcome. However, with more understanding of synthetic and natural biomaterials and the techniques to fabricate the scaffolds, ideal synthetic bone substitutes will be engineered.

The most common biomaterials for scaffolds currently under investigation are polymers, ceramics, and composites of both. These materials can be manipulated into three-dimensional constructs with mechanical integrity, biocompatibility, and osteoconductivity to promote specific cellular activities for bone healing and repair. The architecture and functionality of the constructs can vary from sponges to injectable gels to sintered microspheres depending on the material and techniques used.³² The variations in biomaterials and fabrication methods allow for controllability in design specifics to engineer scaffolds particular to orthopedic applications. Recent advancements showed that the incorporation and controlled release of growth factors, cytokines, and other molecular agents from scaffolds of varying materials have been shown to make materials

osteoinductive thereby improving their bioactivity in facilitating localized bone regeneration.^{11, 12, 33-37}

a. Ceramics

Ceramics are inorganic and nonmetallic substances that have high compressive strength due to the crystalline microstructure. Calcium phosphate, calcium sulfate, and bioactive glass are some ceramics being examined as constructs for bone regeneration as well as drug delivery vehicles because of their high binding affinity for proteins and osteoconductive environment for host bone cells to regenerate bone.¹⁶ Calcium phosphate and bioactive glass are biomimetic since they stimulate the production and deposition of calcium phosphate in solution to improve integration during bone regeneration.¹⁶ Even though calcium phosphate is a major component of bone's mineral phase, it is still a ceramic and when used alone its high resistance to deformation causes it to be brittle and difficult to amend into strong porous constructs.³⁸

In bone tissue engineering, calcium phosphate is commonly used as bone cement due to its injectability, biomimetic characteristics, and osteointegration. The calcium phosphate cement can be transformed into porous hydroxyapatite scaffolds using a particle leaching method but its compressive strength is limited to ~6MPa which is weaker than cancellous bone and prone to scaffold collapse.^{39, 40} The brittleness of the calcium phosphate significantly lowers its compressive strength when porosity is introduced. Therefore, calcium phosphate nanocrystals are commonly mixed uniformly within the construct to enhance implant integration and bone healing while providing compressive strength to provide mechanical support and maintain fracture space.²³

b. Polymers

To avoid the brittleness of ceramics, some bone scaffold investigations focused on polymers for its general material toughness. There are many synthetic polymers (polylactide-*co*-glycolide (PLGA), polycaprolactones, polyanhydrides, etc) and natural polymers (type I collagen, hyaluronic acid, and chitosan) that have been studied for use as scaffolds for bone tissue engineering.^{36, 41-45} These polymers exhibit mechanical stability, biodegradability, and ductility for bone tissue engineering. Some synthetic polymers allow for controllability in degradation, porosity, and mechanical properties while natural polymers provide better cytocompatibility and bioactivity. However, some synthetic polymers have undesirable acidic degradation products and low cytocompatibility while natural polymers have limited controllability in degradation and mechanical strengths.⁴³

For example, in a study performed by Wu and Ding, PLGA produced acidic by-products. Three different compositions of PLGA were compared for mechanical strength and molecular weight during degradation in phosphate buffered saline.⁴³ Their results showed that despite maintaining good compressive strength over the duration for the study, the degradation of PLGA produced by-products causing a decrease in pH from ~7.0 to ~3.0, which raised concerns about decreasing cell viability.⁴³ Consequently, to improve biodegradation and cytocompatibility, Wu et al. coated PLGA scaffolds with collagen and chitosan. The PLGA coated with collagen did improve degradation and those coated with chitosan expressed higher ALP levels. The collagen coating made the scaffold more hydrophilic inducing water absorption which increases the degradation of the PLGA along with lactic and glycolic acid by-products. The PLGA coated with

chitosan, on the other hand, supported osteoblastic expression of extracellular matrix in human bone cells.⁴⁶ Furthermore, PLGA is commonly used with a natural polymer or a ceramic coating to enhance biodegradation, biocompatibility, and osteoconduction.^{43, 44, 46}

Therefore, natural polymers with inherent biodegradability and biocompatibility are of high interest for bone tissue engineering investigations. Chitosan is natural polymer with favorable material characteristics for bone scaffolds including controlled degradation, cationic properties for protein affinity, and solubility in dilute acids for versatile matrix constructs.^{32, 47} However, chitosan does lack mechanical strength. Consequently, to incorporate the advantage of the biomimetic and high compressive property of ceramics, and the toughness and biodegradability of polymers, composite materials of ceramic reinforced polymers are utilized to construct scaffolds with the appropriate physiochemical and mechanical properties similar to that of bone.^{1, 3, 16}

c. Composites

Bone is composed of an inorganic mineral and an organic matrix phase organized into a complex 3D hierarchy structure that no one material can purely be used to replicate and mimic.³¹ Therefore, many bone scaffold designs have integrated osteoconductive calcium phosphate ceramics with natural biodegradable polymers to simulate calcium phosphate reinforced collagen bone composite.^{1, 4, 5, 17}

For example, to improve compatibility of PLGA scaffold materials, Jiang et al. constructed a microsphere-based composite (natural polymer to synthetic polymer) scaffold of chitosan-poly (lactic acid glycolic-acid) (PLGA). Chitosan was used to provide enhanced compatibility while taking advantage of the strength properties of the

PLAGA material. Compared to PLAGA alone the composite chitosan-PLAGA showed enhanced differentiation of an osteoblastic cell line (osteinduction).⁴⁸

Most commonly, ceramics are used with polymer reinforcement to mimic the collagen reinforced hydroxyapatite composite structure naturally found in bone.² In a study performed by Kim et al., the comparison of gas foaming/particle leaching (GF/PL) to solvent casting/particle leaching (SC/PL) was determined in the fabrication porous composite constructs of PLGA and hydroxyapatite (HA). The bone regeneration was examined *in vitro* and *in vivo* for GF/PL, SC/PL, and PLGA with no HA scaffolds. The study concluded that scaffolds fabricated using the GF/PL method had higher HA exposure and in turn led to better bone formation compared to the SC/PL method by two fold and PLGA without HA by ten-fold.⁴¹ However, the unattractive properties of synthetic polymers namely acidic degradation products can over shadow for the biomimetic ceramic and hinder the composite material in bone healing.

The use of a natural ceramic like calcium phosphate mineral toughened by a natural polymer like chitosan may induce better mimicry because of its natural biodegradability and biomimetic ability. Some studies have shown that integration of calcium phosphate with chitosan had about a two-fold increase in compressive strength, cell attachment, and matrix production.^{39, 45, 49-51}

Composite Chitosan-Calcium Phosphate Scaffolds

Chitosan is the natural polymer of interest in this study due to its biocompatibility (causes no inflammation and has antibacterial activity) and biodegradability (nontoxic products of degradation).^{32, 47} Chitosan is the deacetylated derivative of chitin which is

the major polysaccharide matrix polymer component of the exoskeleton of crustaceans, insects, and some fungi. The chemical structure of chitosan is a linear β -(1-4) polysaccharide consisting of glucosamine and *N*-acetyl glucosamine.⁴⁷ The ratio of glucosamine to *N*-acetyl glucosamine determines the degree of deacetylation (DDA). The DDA ranges from 30-95% inversely related to degradation rate (e.g. the higher the DDA the slower the degradation).^{32, 52}

The amino and hydroxyl groups give chitosan its solubility in dilute acids (pH<6.0) and cationic property which allow for the fabrication of various 3D matrix forms with affinity for anionic molecules including glycosaminoglycans (GAG), proteoglycans, proteins and biological agents.^{32, 53} Variability in fabrication techniques can produce 3D constructs of many forms including injectable gels, sponges, porous scaffolds, and microspheres that can serve as a drug delivery vehicle for osteoinductive enhancements with growth factors, cytokines, and other biological agents.⁴⁷ A study conducted by Lee et al., used chitosan sponges loaded with platelet-derived growth factor-BB to demonstrate the osteoconduction and osteoinduction of the chitosan matrix in an *in vitro* and *in vivo* evaluation.⁵⁴ These intrinsic material properties of chitosan are of high interest in bone tissue engineering scaffold design and fabrication.

In bone tissue engineering applications, chitosan is commonly used as a composite with calcium phosphate since both are biocompatible, and osteoconductive, and the calcium phosphate can provide strength while the chitosan provides toughness.^{16, 32} For example, in a comparison of pure chitosan and composite chitosan-calcium phosphate sponge (chitosan based with powder calcium phosphate particles), a two-fold higher compressive strength and 1.5 improvement in cell proliferation and mineralization

was exhibited for the composite sponge.⁴⁹ Xu et al. constructed macroporous chitosan-calcium phosphate scaffolds (calcium phosphate cement based with 1-2% chitosan) with the fast setting capability that could facilitate better bone tissue and implant integration *in vivo* compared to calcium phosphate cement alone.⁵⁵ These studies produced scaffolds exhibiting good pore sizes ~50-120 μ m (Thien et al.) and porosity 52-75% (Xu et al.) along with improvement in mechanical properties with maximum compressive modulus at ~9KPa (Thien et al.) and scaffold strength of 0.3MPa at 65% porosity (Xu et al.).^{49, 55} However, overall mechanical properties remained low when compared to the compressive strength of cancellous bone 10MPa to 2000MPa since there was no direct bonding of calcium phosphate to chitosan chains for mechanical reinforcement.

To improve mechanical properties, a microsphere-based scaffold design based on nanocrystalline calcium phosphate particles homogenous with chitosan have been made.^{45, 50} The architectural design of a microsphere-based scaffold with interconnected pores relies on the fusion of uniform microspheres, which allows for shape and size versatility. This expands the uses of the composite chitosan-calcium phosphate scaffold to a range of orthopedic applications including craniofacial augmentation and long bone fractures. When the microspheres are fused together, a network of interconnected pores are produced to serve as a negative template for efficient nutrient and waste exchange, vascular formation, mechanical integrity, and tissue infiltration. However, current microsphere designs of PLGA and chitosan use a sintering process that exposes the scaffolds to high heat for extended periods, which would alter molecular structure of chitosan. Also the fused connections between the beads were cracked leading to loss of mechanical strength.⁵⁶ Therefore, the composite chitosan and calcium phosphate

microsphere produced from a co-precipitation method can be fused by partially dissolving the surfaces of the microspheres and also eliminate the harsh processing conditions and could improve the fusion between the microspheres.

The calcium phosphate and chitosan are co-precipitated in chitosan matrix to mimic natural organic-inorganic structure of bone. The study conducted by Chesnutt et al. showed that the calcium phosphate is uniformly incorporated within the scaffold microspheres in the nanocrystalline form to enhance compressive strength for load bearing.⁴⁵ The composite scaffold exhibited a two-fold increase in compressive modulus along with better cell proliferation and matrix deposition as indicated by increasing trend in ALP and total protein as opposed to the chitosan scaffold. However, the solid homogenous microsphere alone had slow degradation and low porosity that could not simulate the architectural difference of cortical and cancellous bone. In a follow up study conducted by Reves et al., the composite microspheres were lyophilized and exhibited a four-fold increase in surface area, a 50% increase in porosity, and a high absorption potential which could contribute to faster degradation.⁵⁰

The scaffold used in this study will incorporate two types of microspheres with different physical properties formed through two different drying methods – air-dry and lyophilization. The air-dried (AD) microsphere is a solid providing compressive strength and prolonged degradation while the lyophilized (FD) microsphere is hollow, light, and microporous with increased surface area contributing to faster degradation and protein adsorption.^{45, 50} Combinations of these microspheres in different shapes and sizes have the potential to be versatile constructs improving bioactivity for numerous clinical applications in orthopedics.

Summary

Critical size bone fractures and defects that exceed innate physiological healing processes of bone require surgical intervention to induce bone healing utilizing a bone graft.^{8, 17} Autografts and allografts are the most clinically used bone grafts; however, there are limitations associated with their use including limited quantity and loss of bone physiochemical properties. Consequently, bone tissue engineering endeavors focus on designing scaffolds that mimic the regenerative capacity of bone. Researchers investigate the combination of ceramics, polymers, and their composites to produce scaffolds with the biocompatibility, 3D architecture with interconnected pores, biodegradation, osteoconduction, osteoinduction, and biomechanics similar to bone. The scaffold serves as a temporary negative template with mechanical and biological support for bone formation. A composite of chitosan and calcium phosphate microsphere based scaffold has shown much promise as a bone engineering scaffold since it has advantages of cytocompatibility, biodegradability, osteoconduction, and mechanical properties, though the solid composite microspheres did not exhibit ideal degradation and porosity.⁴⁵ Lyophilized microspheres were demonstrated to increase scaffold surface area and porosity which could lead to increased degradation. Therefore, it is hypothesized that using a combination of lyophilized and solid microspheres of chitosan-nanohydroxyapatite will improve scaffold degradation without compromising mechanical or osteogenic properties.

CHAPTER 2: OBJECTIVES AND SIGNIFICANCE

It is hypothesized that using a combination of lyophilized and solid microspheres of chitosan-nanocrystalline calcium phosphate will improve scaffold degradation without compromising mechanical or osteogenic properties

To test this hypothesis the following specific objectives were undertaken:

Objective 1

Design and construct three-dimensional cylindrical chitosan-nanocalcium phosphate microsphere based scaffold for bone tissue engineering using two varieties of composite microspheres (freeze-dried, FD and air-dried, AD). The AD microspheres are used to form an outer surface to provide strength to the scaffold with the interior surfaces composed of the freeze dried microspheres, which provide increased surface area, porosity and degradability. This hierarchical arrangement is used to mimic long bone organization with the AD providing the hard outer shell and the FD the spongy middle similar to cortical and cancellous bone, respectively. The first steps are to

- a) Create a mold for microsphere fusion having a cross sectional area similar to the long bone.
- b) Determine the optimal ratio of FD to AD within the limits of the mold.
- c) Develop a process and technique to fuse FD and AD microspheres.

Objective 2

Evaluate the ability of bone cells to attach, grow and elaborate bone matrix on scaffolds *in vitro*. For this objective,

- a) Bone cell growth will be measured based on DNA quantification.
- b) Alkaline phosphatase (ALP) activity will be measured for bone phenotype and total collagen levels for extracellular matrix production.
- c) Scanning electron microscopy (SEM) will be used to qualitatively view cells and elaborated matrix on scaffolds.

Objective 3

Characterize the biomechanics and biodegradability of the scaffolds during *in vitro* enzymatic degradation. Degradation and compressive modulus is obtained by

- a) Mass change of AD and FDAD scaffolds.
- b) Compression testing of both scaffold types to obtain the compressive modulus.

Significance

This research will provide data on the potential of using a combination of air-dried and freeze-dried microspheres to construct a bone scaffold to mimic the cortical and cancellous architecture of bone, and provide favorable structures for bone cell growth and matrix production while maintaining mechanical strength and enhancing degradation.

The results of this work, if successful, will provide the foundation for additional scaffold design studies *in vivo*, for bone graft use, use in drug delivery, and clinical applications.

**CHAPTER 3: DESIGN AND EVALUATION OF CHITOSAN-CALCIUM
PHOSPHATE SCAFFOLDS CONSTRUCTED FROM AIR DRIED AND
LYOPHILIZED MICROSPHERES**

Duong T. Nguyen¹, Warren O. Haggard¹, Richard Smith², Jonathan D. McCanless¹, Joel D. Bumgardner¹

¹Department of Biomedical Engineering, University of Memphis, Memphis, TN

²Department of Biomedical Engineering and Orthopedic Surgery, University of Tennessee Health Science Center, Memphis, TN

Planned submission to Journal of Biomedical Materials Research A

Abstract

Chitosan nano-hydroxyapatite composite microsphere based scaffolds have exhibited mechanical and osteoconductive properties favorable for use as a bone graft substitute material. However, the degradation of the scaffold has been limited. By incorporating lyophilized microspheres to the scaffold construct, scaffold porosity can increase leading to an increase in scaffold degradation. In this study, scaffolds were constructed from solid air-dried and lyophilized composite chitosan-calcium phosphate microspheres and were evaluated *in vitro* for cell behavior and mechanical properties. The combination scaffold composed of air-dried and lyophilized microspheres (FDAD) was compared to the air-dried scaffold (AD). It was hypothesized that the addition of lyophilized microspheres (FD) would improve scaffold degradation without compromising the osteogenic and mechanical properties of the scaffold. Mineralization results showed FDAD had 80% higher cell number ($p < 0.01$) and 31% greater collagen elaboration as compared to AD. However, the addition of FD microspheres did compromise the mechanical properties decreasing the compressive modulus by 60% without increasing scaffold degradation. These results indicate FDAD scaffolds have more osteogenic potential based on cell growth and collagen elaboration, but AD scaffolds demonstrated higher compressive strength. Even though results did not support the stated hypothesis, further investigations to improve scaffold strength will be conducted for this osteogenic construct.

Keywords: chitosan scaffolds, chitosan microspheres, degradation, compression, mineralization

Introduction

As the ≥ 65 age group reaches its projected 51.5 million in 2020, the number of age-related fractures will significantly increase the current yearly demand of 500,000 bone grafts.^{1, 2} Surgical treatment for bone fractures and defects commonly utilize autografts and allografts. Autografts are bone tissue commonly retrieved from the patients' own iliac crest; however, the quantity and quality of the bone from aged patients are low.³ Allografts are donor bone tissues that have been decellularized to remove all bacterial and viral diseases along with some innate physiochemical and mechanical properties.³⁻⁵ Bone tissue engineering approaches are focused on engineering synthetic scaffolds that can mimic the physiological functions of bone. The scaffolds are engineered to induce osteogenesis by providing a three-dimensional (3D) support environment favorable for osteoblasts to grow, proliferate, and form new bone formation.⁶⁻⁸ The scaffolds serve as functional templates for bone regeneration, provide temporary support within the fracture gap, and are integrated into the body during bone healing and formation.

The current composite materials of high interest are incorporate calcium phosphate, native to bone, with chitosan because of its unique biomaterial properties favorable for bone tissue engineering. Chitosan is a natural polymer, derived from partial deacetylation of chitin, which is a polysaccharide found in the exoskeleton of crustaceans and insects.^{9, 10} The polysaccharide backbone and amino side groups give chitosan its unique properties of controlled degradation, protein affinity, and acidic solubility.⁸⁻¹⁰

Chitosan combined with calcium phosphate in different scaffold designs support increased cell proliferation and mineralization when compared to chitosan and ceramics

alone.¹¹⁻¹³ Xu et al. constructed a macroporous scaffold from a composite of injectable calcium phosphate cement (CPC) and 1-2% of chitosan that showed improved implant integration compared to CPC scaffolds alone but it had limited compressive properties (9MPa at 20% macro-porosity and 2.5MPa at 40% macro-porosity) and degradation was undetermined.¹³ In a different macroporous scaffold design, Thein-Han et al. demonstrated that composite chitosan sponge scaffolds incorporating powder calcium phosphate enhanced cell attachment, proliferation, and good cell morphology with 15-29% degradation but it also had limited compressive properties (maximum ~9KPa).¹¹ Chesnutt et al. incorporated nanocrystalline calcium phosphate with chitosan through a co-precipitation method to produce composite microsphere based scaffolds that exhibited better bone cell proliferation and mechanical properties (~9MPa closer to minimal cancellous strength) than scaffolds constructed from chitosan microspheres.¹⁴⁻¹⁶ However, there was no significant mass change for both scaffold types possibly due to the degree of deacetylation and crystallinity of chitosan and even density of microspheres.¹⁴ In a follow-up study, Reves et al. demonstrated that the surface area, porosity, and absorption of the composite chitosan-calcium phosphate microspheres could increase with lyophilization which could lead to better degradation.¹⁷

The aim of this study is to combine freeze-dried (FD) composite microspheres with solid air-dried (AD) composite microspheres to construct a scaffold that mimics the architecture of long bone while providing mechanical support (10-2000MPa) at the fracture site. It is hypothesized that incorporating FD microspheres will improve scaffold degradation without compromising the mechanical and osteogenic properties. Combination scaffolds (FDAD) of organized FD and AD microspheres were constructed

for *in vitro* mineralization and degradation evaluation to determine osteoblastic attachment and proliferation, scaffold osteoconduction, and compressive modulus change during degradation. All AD scaffolds were used as controls.

Materials and Methods

Fabrication of Composite Chitosan Calcium Phosphate Microspheres

Composite microspheres were produced through a co-precipitation method.¹⁴ Briefly, 87.4% DDA chitosan and calcium phosphate were dissolved in 2% (v/v) acetic acid for 24 hours. Then the solution was filtered through a 200 μ m nylon mesh to remove any large particulates. The microspheres were formed through a co-precipitation process in which the solution is added drop-wise to a strong base solution (50 wt% of distilled water, 30 wt% methanol, and 20 wt% sodium hydroxide). The microspheres were stirred in the base solution for 24 hours to allow for the formation of calcium phosphate nanoparticles. The batch of microspheres was washed with deionized (DI) water with constant stirring and water replacement until the pH reached 7.5-8.0. The microspheres were then dried by two different methods: air-dried and lyophilized (freeze-dried). For the air-dried method, the microspheres were spread out in a single layer and allowed to dry in a fume hood. For freeze-dried method, a majority of the moisture was removed from the microspheres before placing them sparingly on dishes to freeze in the -80°C freezer. Once the microspheres were frozen, after an hour, they were transferred to the lyophilizer (FreezeZone 2.5, Labconco) to freeze-dry overnight.

Fabrication of Scaffolds

The washer-shaped scaffolds were formed by fusing microspheres in a circular mold. The combination scaffold (FDAD) had an outer ring of air-dried (AD) microspheres and an inner ring of freeze-dried (FD) microspheres. The all air-dried scaffolds consisted of only air-dried microspheres. The amount of microspheres for each

scaffold was weighed for consistency both in mass and size. The AD scaffolds were made with 0.610 ± 0.005 g of AD microspheres while the FDAD scaffolds consisted of 0.290 ± 0.005 g of AD microspheres and 0.080 ± 0.005 g of FD microspheres. To fuse the microspheres, about 3-4 drops of 1% acetic acid was used to partially dissolve the surface of the microspheres to make the microspheres adhere to each other. The acid rinsed microspheres were transferred to scaffold molds. The molds were made with ~7mm thick cross sections from 15ml centrifuge tubes (FisherBrand). The molds containing the microspheres were air-dried in a fume hood to remove excess acid.

Scaffold Architecture

Scaffold dimensions (height, outer diameter, wall thickness) were measured using a caliper before compression in the hydrated state. The architecture and surface topography was also examined under SEM.

Cell Culture

Both scaffold types were sterilized using low dose gamma irradiation (25-32 kiloGreys) and then soaked in medium to neutralize any residual acid for 2 days before use with cells. The human sarcoma cell line (Saos-2; ATCC HTB-85) was used to evaluate the ability of the scaffolds to support bone cell growth and matrix production. Approximately two million cells were seeded onto the scaffolds using mineralizing medium (McCoy's 5A Medium with 10mM of β -glycerol phosphate, and 50 μ g/mL of ascorbic acid in addition to 10% fetal bovine serum and 1% antimycotic and antibiotic (Fisher, Penicillin-10,000 IU/mL, Streptomycin-10mg/mL, Amphotericin B-25 μ g/mL).

The medium was changed every 2 or 3 days for 28 days. Representative samples (n=4) of both scaffolds were collected at days 1, 7, 14, 21, and 28 for cell proliferation, amount of ALP, and extracellular collagen measured.

Cell Proliferation

To confirm cell attachment, growth, and proliferation, cell number was measured via DNA quantification for day 1, 7, 14, 21, and 28 for both sample types (n=4). Scaffolds were collected at random for each time point and transferred to new well plates and ultrasonicated for ~10 seconds per side with 2mL of sterile water (Fisher Scientific). The lysate was used for measuring DNA using the Picogreen (Invitrogen, Eugene, OR) assay and alkaline phosphatase activity. The Picogreen reagent is a nucleic acid stain for quantitating double-stranded DNA (dsDNA) in solution, which would correspond with cell number. The concentration of the nucleic acids was determined at an absorbance of 260nm. DNA was reported normalized to scaffold mass. For visual verification, Live/Dead® staining was used for both sample types (n=1). The reagents of the Live/Dead® are calcein, which causes live cells to fluoresce green under blue light, and Eth D-1, which causes dead cells to fluoresce red under green light. The scaffolds with stained cells were viewed using a Nikon Eclipse TE300 with mercury lamp (Southern Instruments, GA) and images recorded XCCD camera and the BioQuant Osteo II software (Nashville, TN) to visualize cell viability and distribution.

Alkaline Phosphatase Activity and Hydroxyproline Content

The lysate collected from scaffolds (n=4) at each time point was used to measure alkaline phosphatase (ALP) enzymatic activity for osteoblastic phenotype expression.

ALP was measured based on the hydrolysis of p-nitrophenyl phosphate following Sigma ALP protocol. Absorbance measurements were taken at 405nm. The ALP activity was computed from the standard curve with duplicates averaged. Amount of ALP normalized to DNA was reported with standard deviations for days 1, 7, 14, 21, and 28.

Collagen concentration was determined by quantifying hydroxyproline, a major component of collagen making up 12.5% of the dry weight of the structural protein. The method used was a modified version of that described by Reddy and Enwemeka¹⁸. Representative samples (n=2, replicates were reduced due to loss of samples) of both scaffold types were collected and weighed to normalize hydroxyproline to scaffold mass (μg of collagen/ g of scaffold). The samples were transferred into microcentrifuge tubes (Thermo Fisher Scientific, Inc.), which contained o-rings inside the caps to withstand positive pressure. Teflon tape was also applied to the threads of tubes for reinforcement. Amino acid hydrolysis was conducted using 1.5 mL of 6M HCl into each tube and the tubes placed inside a high heat resistant glass bottle to equalize pressure during the incubation at 110°C overnight. The samples were allowed to cool before they were centrifuged for 10 minutes at 14,000 RPM to separate the particulates from the aqueous solution containing the hydroxyproline. The 1mL of the aqueous solution was transferred to 25mL Erlenmeyer flask with 4mL of DI water. The samples were then prepared for lyophilization to concentrate the hydroxyproline. Lyophilization was repeated once more after rehydrating with 4ml of DI water to reduce the acidity. Additionally, hydroxyproline (Sigma-Aldrich) standards were made in DI water and subjected to hydrolysis. Each supernate (25 μl) was tested in duplicates using the chloramine-T oxidation of hydroxyproline to a pyrrole derivative followed by chromogen production with the

addition of Erhlich's reagent in a 96-well culture plate. Absorbance measurements were taken at 550nm using a SpectraMax[®] Plus³⁸⁴ spectrophotometer (MDS Analytical Technologies, Inc., Toronto, Canada). Background measurements taken at 550nm were subtracted and standard curves were generated to determine unknowns. Specimen values were taken as the average of the duplicates.

Extracellular Matrix Production

SEM images were qualitatively examined for cell proliferation, morphology and matrix production. Samples for the SEM were prepared according to protocol by soaking the scaffolds in 4% formalin overnight and into consecutive ethanol solutions 70, 80, 90, and 95% for 15 minutes each and then twice in 100% ethanol for 1 hour. The scaffolds were sputter coated with 70nm of gold and platinum to be viewed in environmental SEM (Philips ESEM30) at 30kV.

Enzymatic Degradation

In vitro degradation was simulated using a lysozyme and sterile DI water solution. Initial dry mass (mg) of AD and FDAD scaffolds was obtained before the scaffolds were packaged for gamma irradiation. The scaffolds were contained in a 12-well plate then soaked in 3mL of 100µg/ml lysozyme (MP Biomedicals, OH) in water. The lysozyme solution was changed every 2 days. Samples (n=4) of AD and FDAD were collected at days 1, 7, 14, 21 and 28 and compression testing was conducted before final dry weight was obtained (see section 3.3.9). Once the scaffolds were mechanically tested, the scaffolds were placed into a vacuum oven to dry under vacuum pressure of 15psi and at a

temperature $\sim 37^{\circ}\text{C}$ for 5 days. Percent change in mass was calculated based on the initial pre-sterilization dry mass and final dry mass of compressed scaffolds (dried under vacuum at 37°C).

Compression Testing

Compression testing was conducted using an Instron mechanical testing machine (Model: 33R, MA) and the integrated Bluehill software. Hydrated scaffolds collected during days 1, 7, 14, 21, and 28 of degradation ($n=4$) were compressed under a 5kN load cell at a controlled rate of 1mm/min until 50% compressive strain. Testing specimen was specified as tubular (outer diameter, wall thickness, and height) and dimensions for each cylindrical scaffold were used. Compressive modulus and compressive stress at 50% strain were determined using the Bluehill software. Data were collected at days 1, 7, 14, 21, and 28 of degradation.

Statistical Analysis

This study compared AD scaffolds versus combination FDAD scaffolds using two-factor (scaffold type, time) ANOVA (Microsoft Excel) with SNK post-test to determine significance and differences. Significance was declared at $p < 0.05$.

Results

Scaffold Architecture

Consistency and similarity in the shape of each microsphere type and dimensions within the scaffold types can be seen in the dimension data (Table 1). The scaffolds are cylindrical in shape with a hollow center core. The FDAD scaffold has an outer shell of AD microspheres and an inner core of FD microspheres to simulate the arrangement of long bone.

The orange arrow in Figure 1 demonstrates the surface area where two AD microspheres were fused together. This area is difficult to see on FD microspheres due to the textured surface. Microsphere surface topography is apparent at 25x magnification under SEM. SEM micrographs show a smooth surface for AD microspheres and the textured surface of the FD microsphere. Sectioned AD microspheres show homogenous core while the FD microspheres are porous (Figure 1).

Table 1. Summary of Scaffold Dimensions (mm)

Parameters	AD Scaffolds (n=20)	FDAD Scaffolds (n=20)
Outer Diameter	15.86 ± 0.13	14.94 ± 0.12
Wall Thickness	5.63 ± 0.14	5.13 ± 0.14
Height	7.33 ± 0.04	6.81 ± 0.17

AD scaffolds – scaffolds constructed from solid air-dried microspheres

FDAD scaffolds – scaffolds constructed from solid air-dried and freeze-dried microspheres

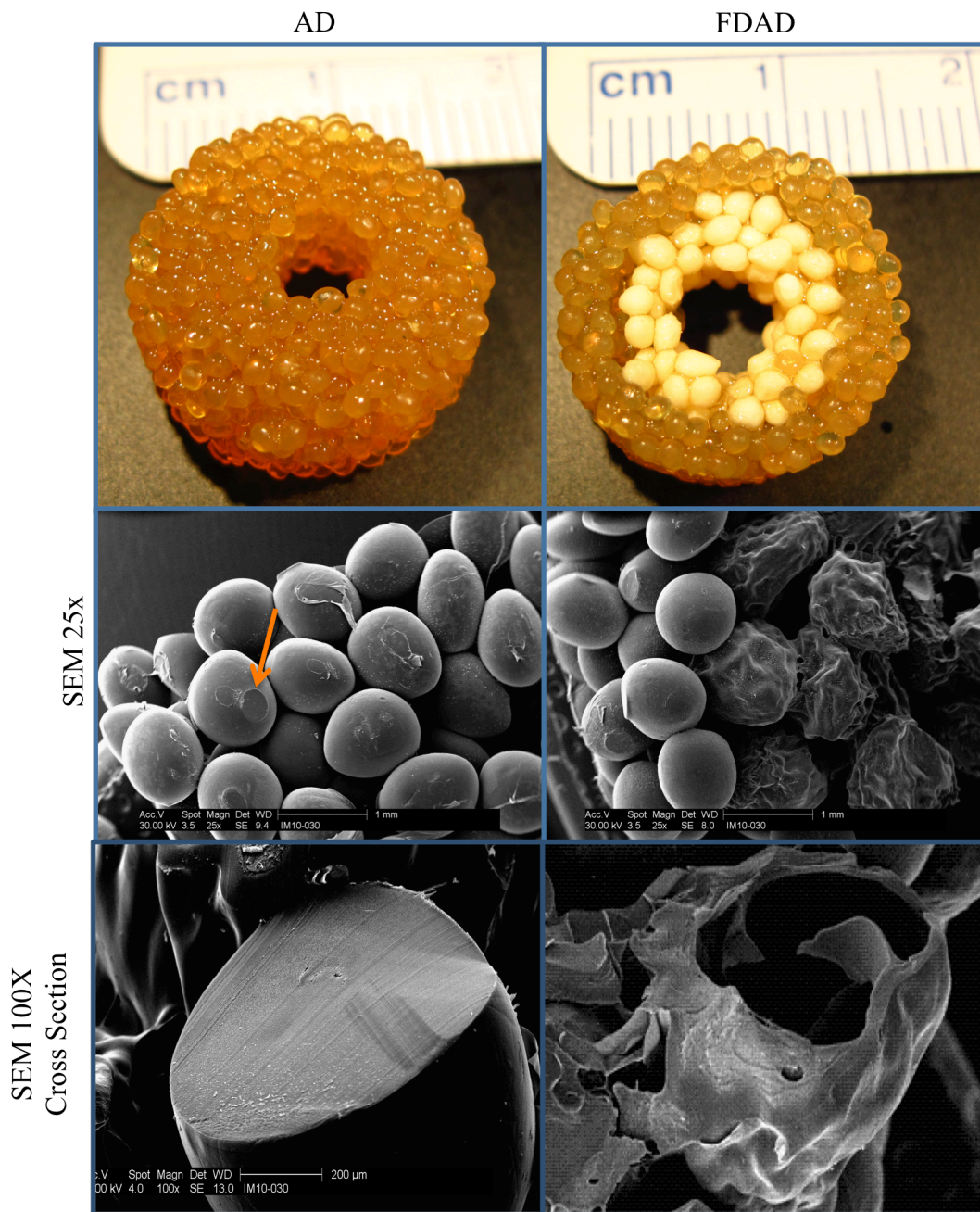


Figure 1. Images of the AD scaffold (left) and FDAD combination scaffold (right) are shown. At 25x, the SEM images show the smooth surface of air-dried (left) microspheres and the highly rough topography of the lyophilized microspheres (right). Orange arrow points to fusion area between two microspheres. Cross sections of AD and FD microspheres at 100x shows the interior solid and hollow core, respective.

Qualitative Microscopy

Live/Dead® images show live cells as green and dead cells as red. Few dead cells, that indicated high cell viability, was present on all scaffolds at all time points. Based on fluorescent images, similar cell attachment and proliferation were seen for both scaffold types at all time points at 40x magnification. Saos-2 cells appeared to localize at microsphere contact points on the AD scaffolds indicated by the white arrows (Figure 2). The textured surface of the freeze-dried microspheres in the FDAD scaffolds created a favorable environment for cell attachment across the surface.

SEM images show cell morphology varied from elongated and flat to circular and spherical (Figure 3). The variation in cell morphology can be seen uniformly throughout the scaffold at all time points and with no preference to area. Minimal matrix deposition on the scaffolds over the 28 day cultures was seen via SEM examination (Figure 3).

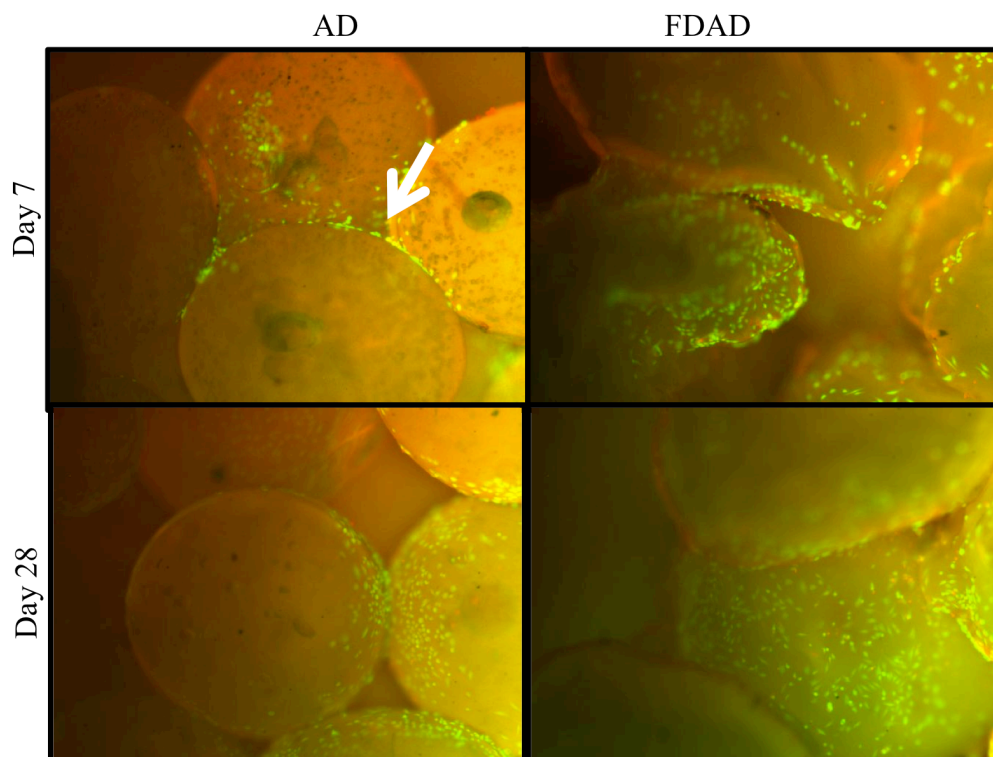


Figure 2. Fluorescent images of scaffolds stained with Live/Dead® to show green fluorescing live cells and red fluorescing dead cells at 40x magnification. Representative fluorescent images are overlay images of the sample under green and red fluorescence. White arrow indicates microsphere contact point with high cell concentration.

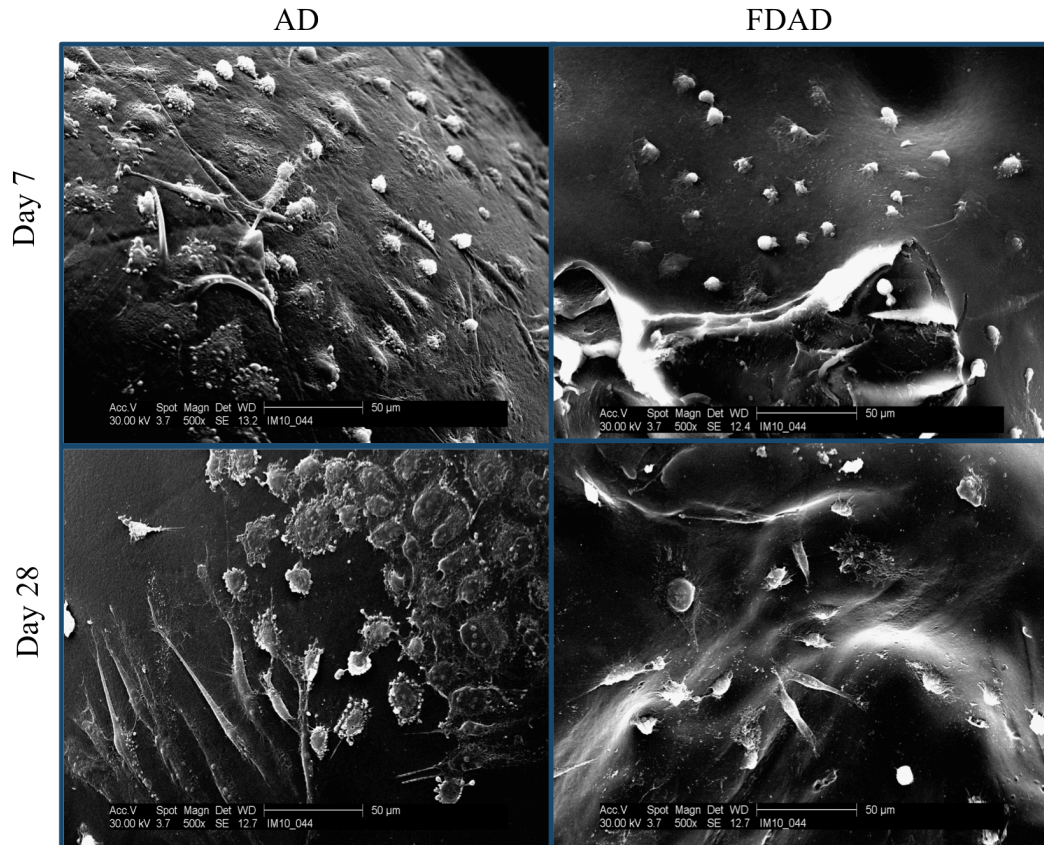


Figure 3. SEM images of AD and FDAD scaffolds at different time points of mineralization. Variation of cell morphology can be seen at 500x magnification.

DNA quantification and ALP Activity

Two-factor ANOVA indicates a difference in DNA concentration over time ($p < 0.001$) and between scaffold types ($p < 0.001$). Post-hoc analyses indicate that FDAD scaffolds had significantly higher cell number (~31%) than AD scaffolds at all time points (Figure 4). For FDAD scaffolds, cell number remains relatively constant from day 1 to 7, increases significantly from day 7 to 14, plateaus between day 14 and 21, and then decreases slightly but not significantly at day 28. For AD scaffolds, while there was a trend for increasing cell number over 28 days, increases were not statistically significant.

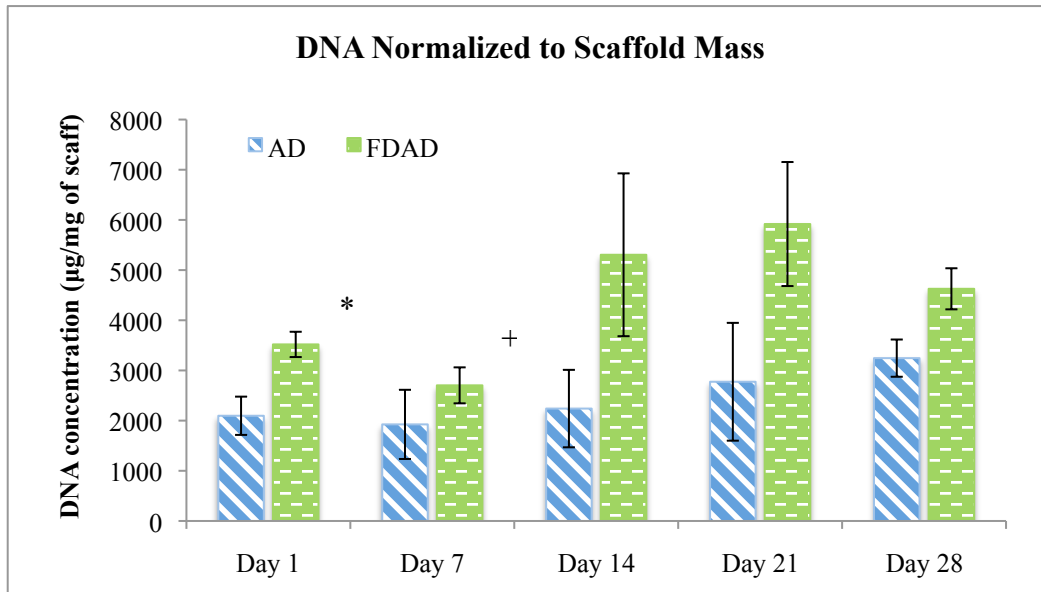


Figure 4. DNA concentration is an indicator of the number of cells during 28 days of mineralization. DNA is normalized to scaffold mass for comparison between the two scaffold types. There is a significant difference between scaffolds types ($p < 0.001$) at all time points. + Significantly different from other days except day 1, * Significantly different from days 21, and 28.

Two-factor ANOVA of ALP levels indicates a difference in ALP levels over time ($p = 0.002$) but no difference between scaffold types. Post-hoc analyses reveal significant changes in ALP levels only for FDAD scaffolds (Figure 5). ALP levels decrease from day 1 to 7, increase significantly from day 7 to 21, and then decrease slightly but not significantly from day 21 to 28. For AD scaffolds, while there was a similar trend in ALP levels over the 28 days, changes were not statistically significant.

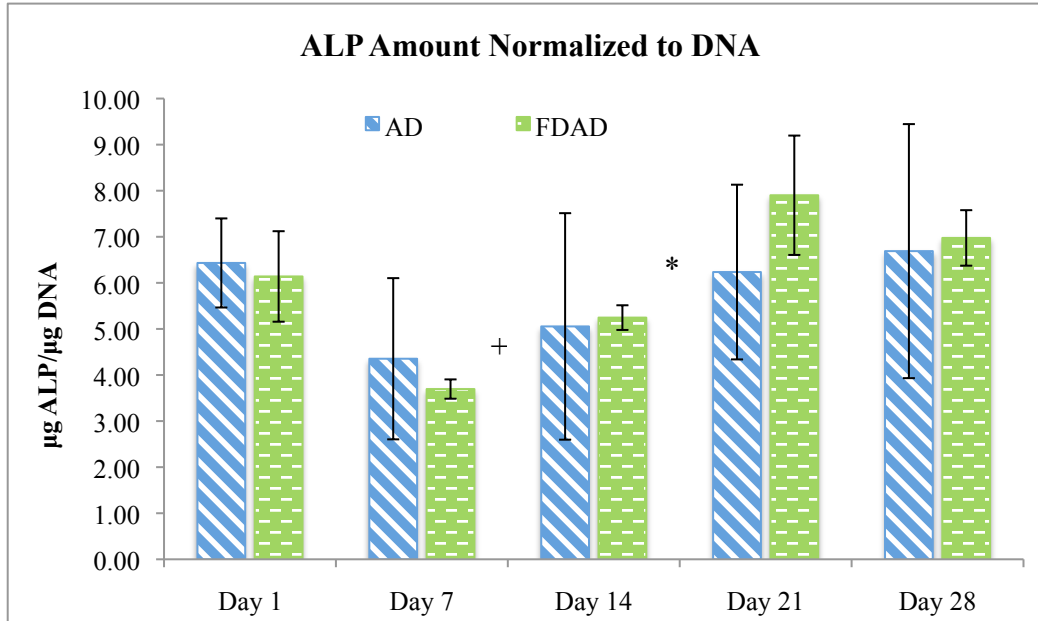


Figure 5. Alkaline phosphatase activity normalized to DNA concentration for osteoblast phenotypic expression. No significant difference between scaffold types. There is a significant difference over time ($p=0.002$). + Significantly different from other days except 14. * Significantly different from days 21 and 28.

Hydroxyproline Content Normalized to Scaffold Mass

Total collagen based on determination of hydroxyproline production on AD and FDAD scaffolds exhibits no difference over time but a difference between scaffold types ($p=0.0067$) (Figure 6). On average, 80% more collagen was produced on FDAD scaffolds than on AD scaffolds. However, cells on the FDAD scaffolds was ~31% greater than on the AD scaffolds.

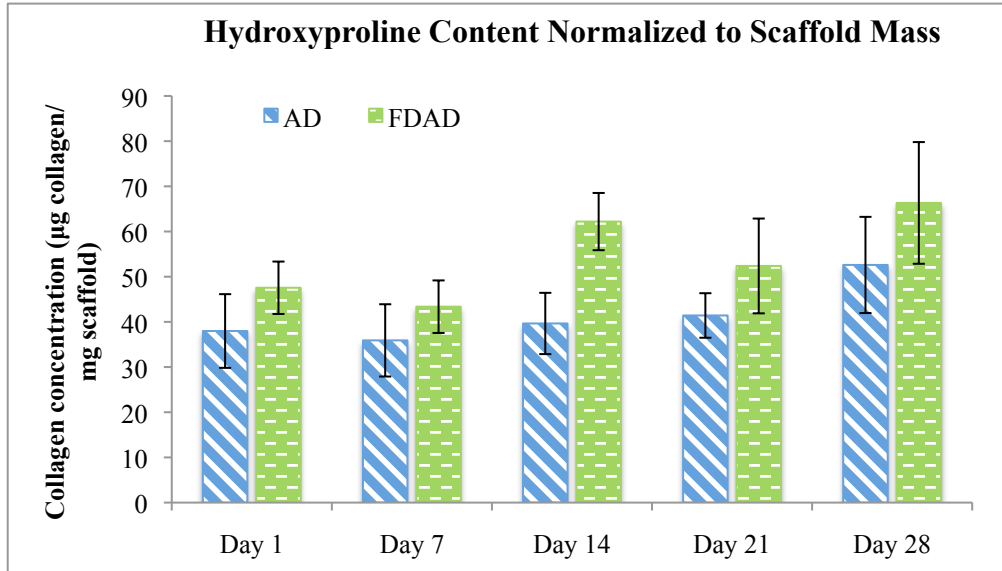


Figure 6. Hydroxyproline content measurements during mineralization as an indicator of collagen synthesis. Significant difference between scaffold types ($p=0.0067$).

Degradation and Compression

Data on the degradation of the scaffolds based on change in mass is shown in Figure 7. Graph shows mass gain (positive percent) and mass loss (negative percent). The pattern of mass change is irregular and standard deviations are wide. At day 1, the AD scaffolds exhibited 2-17% range of mass gain as opposed to the 2-4% mass gain of the FDAD scaffold. Then at day 21, mass of AD scaffolds had no change to a 6% loss in mass. By day 28, there was mass gain. Consequently, there were no difference between scaffold types and with time.

Compressive strengths for both scaffolds exhibit no significant change over time. However, as shown in Figure 8, the compressive moduli for AD scaffolds were significantly higher than the FDAD scaffolds ($p<0.001$) (Figure 8). At day 7, AD scaffolds demonstrated a maximum average modulus of 12.5 ± 2.8 MPa as oppose to

FDAD scaffolds with an average of 2.2 ± 1.4 MPa. Over the 28 days of degradation, the compressive moduli of both scaffolds showed no significant change.

During compression testing of the FDAD scaffolds, visual observation of the stress and strain curve showed an initial rise in the stress strain curve supported by the exterior shell of AD microspheres and slight decrease in stress when the AD shell was broken.

Figure 9 showed a FDAD scaffold before and after compression. The outer AD microsphere shell was permanently deformed while the interior FD microspheres exhibited no permanent deformation.

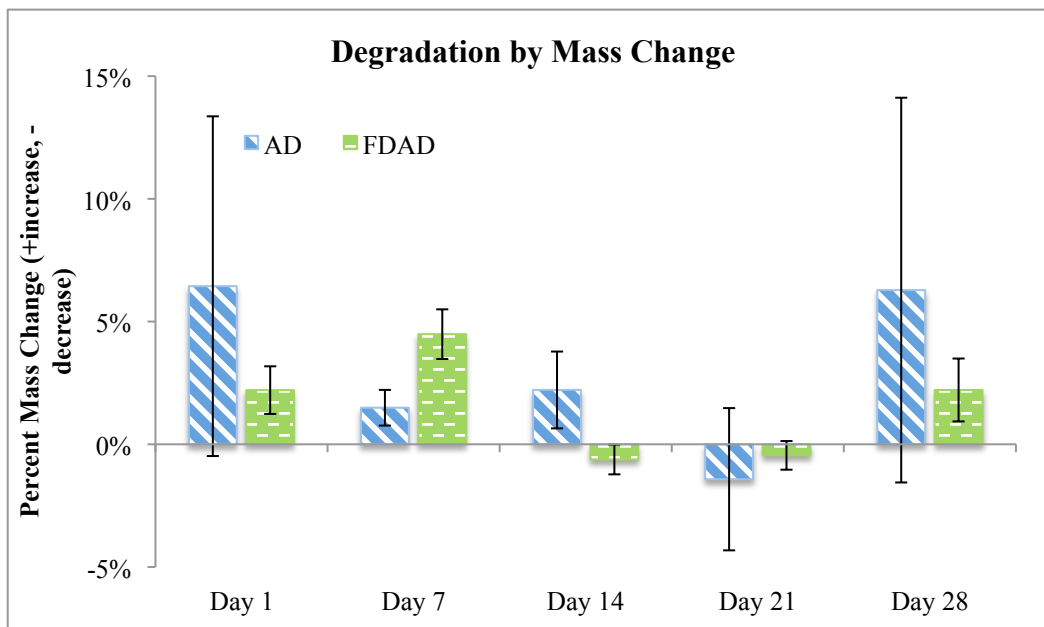


Figure 7. Mass change of AD and FDAD scaffolds (n=4) during enzymatic degradation for 28 days. No significant difference between scaffold types and with time.

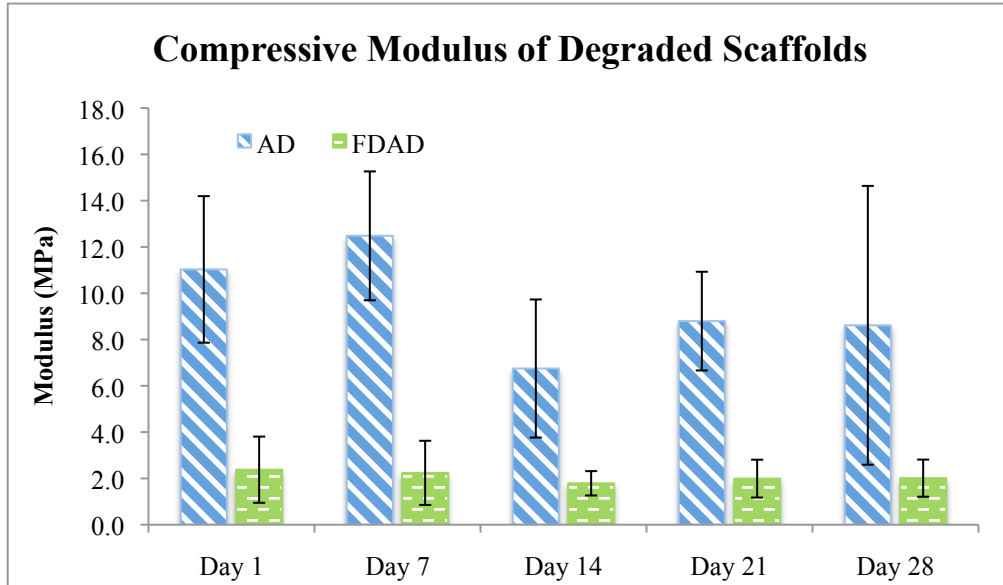


Figure 8. Compressive modulus of scaffolds (n=4) at different time points of lysozyme degradation. There is no change in compressive modulus for bone scaffold types. Significant difference between scaffold types ($p < 0.001$).

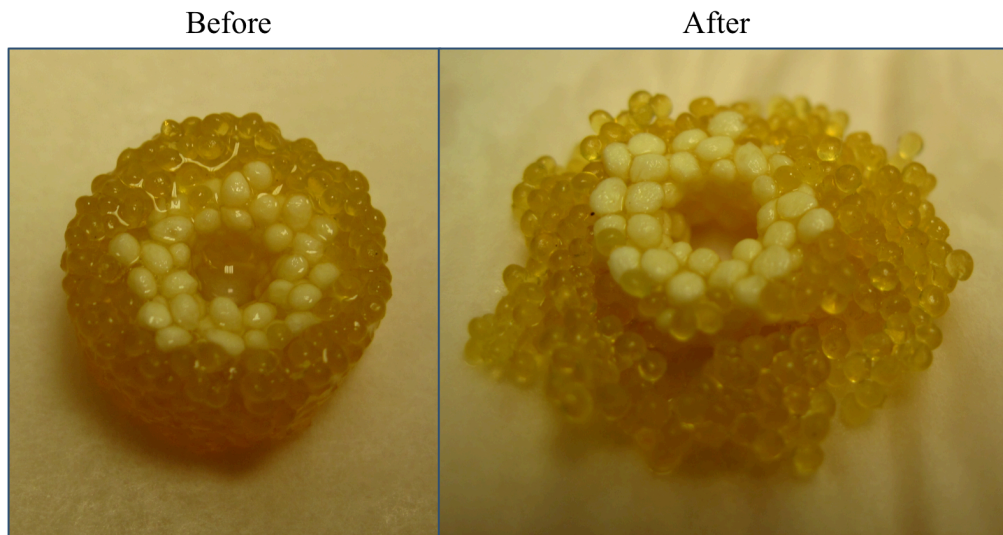


Figure 9. FDAD scaffolds before and after compression testing. The exterior AD microspheres were deformed while FD interior had no permanent deformation.

Discussion

Composite chitosan-calcium phosphate macroporous scaffolds produced by Xu et al. and Thien-Han et al. were composite mixtures based on CPC with small amounts of chitosan and chitosan based with powder calcium phosphate particles, respectively.^{11, 13} The scaffold mechanical properties were characterized and results demonstrated a flexural strength of ~9MPa at 20% macro-porosity and ~2.5MPa at 40% macro-porosity (Xu et al.) and a compressive modulus of ~9KPa (Thien-Han et al.) which is low when compared to the porosity (75-95%) and compressive modulus (10-2000MPa) of cancellous bone.^{11, 13, 15} The composite microsphere-based scaffolds produced by Chesnutt et al. provided compressive strength (~9MPa) and porosity (33-35%) more similar to cancellous properties. However, the microspheres exhibited no mass loss during 14 days of enzymatic degradation.¹⁴ Reves et al. produced freeze-dried microspheres and constructed a microsphere-based scaffold with increased porosity by 50% and surface area by 400% as compared to an all air-dried scaffold similar to those constructed by Chesnutt et al.^{14, 17}

To take advantage of the mechanical properties of the microsphere-based composite chitosan calcium phosphate scaffolds and the increased porosity, and surface area of the freeze dried microspheres, this study created a novel scaffold design incorporating both solid AD and hollow FD microspheres for mechanical stability and increased surface area for more efficient degradation. The design of the scaffold is similar to that of a cross section of long bone. The scaffold was evaluated via *in vitro* mineralization and degradation to determine osteoblast growth and mineralization, and

compressive modulus change during degradation. Results were compared to all AD microsphere based scaffolds.

FDAD scaffolds supported growth and expression of bone cells, markers, and matrix proteins during 28 days of *in vitro* mineralization. Furthermore, FDAD scaffolds showed 31% higher cell number per scaffold mass leading to an 80% greater collagen elaboration per scaffold mass as compared to AD scaffolds. Cell numbers were higher because FD microspheres had textured surfaces and hollow cores, which are indicative of increased surface area and decreased density, respectively. While cells elaborated collagen and cells on FDAD elaborated more collagen than AD scaffolds, significant mineralized matrix was not observed on scaffolds similar to what others have seen.^{11, 14, 19} Cell to cell contact is critical to matrix production and mineral deposition but cells were not confluent on the scaffolds which could hinder mineralization.

The low cell confluence may also be the reason to delayed peak ALP expression on the scaffolds as compared to past studies. Typically, ALP peak occurs around day 7-14 of mineralization but in this study the peak was not seen until day 21.²⁰ Since the peak ALP expression is associated with the onset of mineralization, the delay in expression would be indicative of why extensive mineralized matrix was not observed within the study time frame.

The degradation of the scaffolds as estimated by change in mass did not reveal any substantial change in scaffolds. Similarly, there were no changes in mechanical properties of the scaffolds over time. These data would suggest that despite the presence of lysozyme in solution, there was little if any degradation of the scaffolds. The low degradation may be attributed in part to the relatively high degree of deacetylation

(DDA) of the chitosan. Chitosans with high DDA typically have high crystallinity, and show resistance to enzymatic attack hence the higher the DDA the slower the degradation. Even with the addition of FD microspheres, FDAD exhibited minimal mass loss. However, this may also be an issue with the measurement for mass loss since initial moisture content of scaffolds were not controlled prior to starting experiments. Also, even if FD microspheres degraded, relative change in mass may not be easily determined by mass loss. However, minimal loss in mass and mechanical properties over the 4 weeks may be advantageous since only newly formed, immature bone is regenerated within that time frame, hence, without sufficient mechanical integrity additional support is required to prevent collapse of the scaffold and new bone. A longer degradation study could determine when degradation is initiated along with mechanical loss. Jiang et al. demonstrated that the sinter PLGA and chitosan microspheres had no dramatic decrease in mass, molecular weight, or mechanical strength after 12 weeks even though the *in vivo* rabbit study showed good bone formation for the composite scaffolds.²¹ The FDAD scaffold design did not improve degradation but it did improve cell attachment and collagen production.

Jiang et al. constructed scaffolds based on sintered composite PLGA-chitosan microspheres reported a compressive modulus ranging from ~220-440 MPa (hydrated or dry was not stated) depending on the temperature and duration of sintering.²² Chesnutt et al. used similar composite chitosan calcium phosphate microspheres to construct scaffolds having a maximum modulus of 9.28 MPa when hydrated and 117.57 MPa when dry.¹⁴ This study only conducted mechanical testing on hydrated scaffolds but in a follow up study compression testing should be conducted for the dry scaffolds to determine how

much mechanical strength is lost during hydration and also to compare to dry and hydrated bone strength. The hydrated AD scaffolds demonstrated similar compressive modulus of 9.5 MPa which is comparable to that of cancellous bone (10-2000 MPa) while FDAD scaffolds exhibited an average modulus of 2.1 MPa. The inner FD microspheres were elastic due to its porous structure since no permanent deformation was seen after compression. As for the AD scaffolds, the microspheres after compression were separated from one another but more so after day 7. Consequently, the fusion between FD microspheres as opposed to AD microspheres were stronger and more integrated. Even though the addition of FD microspheres reduced mechanical strength, fracture treatments use bone grafts in conjunction with internal fixation devices to transmit the majority of the load. Furthermore, incorporating FD microspheres showed an improvement in osteoconduction.

Conclusion

In this study, FDAD scaffold design incorporated air-dried and freeze-dried composite chitosan calcium phosphate microspheres to provide mechanical support similar to cancellous bone, and degrade without substantial loss in mechanical integrity. Both scaffolds exhibited cytocompatibility but FDAD scaffolds allowed for higher cell number per scaffold mass. Consequently, FDAD scaffolds had higher total collagen production based on scaffold mass than AD scaffolds. The degradation of AD and FDAD scaffolds over a 4 week test period in lysozyme was minimal. In compression testing, the AD scaffolds exhibited greater compressive strength than FDAD scaffolds. Even though the incorporation of FD microspheres compromised mechanical integrity of the FDAD

scaffold, osteogenic properties were improved with higher cell population and production of collagen content as compared to scaffolds with AD scaffolds. Future studies will focus on characterizing pore size, porosity, and surface, improving the rate of degradation, and maximizing compressive modulus of the combination FDAD scaffolds to serve as bone graft substitutes.

References

1. Koo DA, D.; Copeland, T.; Hall, P. Incidence and Costs to Medicare of Fractures Among Medicare Beneficiaries Aged ≥ 65 Years — United States, July 1991–June 1992: Centers for Disease Control and Prevention; 1996.
2. Lewandrowski KU, Gresser JD, Wise DL, Trantol DJ. Bioresorbable bone graft substitutes of different osteoconductivities: a histologic evaluation of osteointegration of poly(propylene glycol-co-fumaric acid)-based cement implants in rats. *Biomaterials* 2000;21(8):757-64.
3. Khan SN, Cammisa FP, Jr., Sandhu HS, Diwan AD, Girardi FP, Lane JM. The biology of bone grafting. *J Am Acad Orthop Surg* 2005;13(1):77-86.
4. De Long WG, Jr., Einhorn TA, Koval K, McKee M, Smith W, Sanders R, et al. Bone grafts and bone graft substitutes in orthopaedic trauma surgery. A critical analysis. *J Bone Joint Surg Am* 2007;89(3):649-58.
5. Burchardt H. The biology of bone graft repair. *Clin Orthop Relat Res* 1983(174):28-42.
6. Khan Y, Yaszemski MJ, Mikos AG, Laurencin CT. Tissue engineering of bone: material and matrix considerations. *J Bone Joint Surg Am* 2008;90 Suppl 1:36-42.
7. Langer R, Vacanti JP. Tissue engineering. *Science* 1993;260(5110):920-6.
8. BarrÈre FM, T.A.;de Groot, K.;van Blitterswijk, C.A. Advanced biomaterials for skeletal tissue regeneration: Instructive and smart functions. *Materials Science and Engineering: R: Reports* 2008;59(1-6):38-71.
9. Di Martino A, Sittinger M, Risbud MV. Chitosan: a versatile biopolymer for orthopaedic tissue-engineering. *Biomaterials* 2005;26(30):5983-90.

10. Khor E, Lim LY. Implantable applications of chitin and chitosan. *Biomaterials* 2003;24(13):2339-49.
11. Thein-Han WW, Misra RD. Biomimetic chitosan-nanohydroxyapatite composite scaffolds for bone tissue engineering. *Acta Biomater* 2009;5(4):1182-97.
12. Shi C, Zhu Y, Ran X, Wang M, Su Y, Cheng T. Therapeutic potential of chitosan and its derivatives in regenerative medicine. *J Surg Res* 2006;133(2):185-92.
13. Xu HH, Simon CG, Jr. Fast setting calcium phosphate-chitosan scaffold: mechanical properties and biocompatibility. *Biomaterials* 2005;26(12):1337-48.
14. Chesnutt BM, Viano AM, Yuan Y, Yang Y, Guda T, Appleford MR, et al. Design and characterization of a novel chitosan/nanocrystalline calcium phosphate composite scaffold for bone regeneration. *J Biomed Mater Res A* 2009;88(2):491-502.
15. Athanasiou KA, Zhu C, Lanctot DR, Agrawal CM, Wang X. Fundamentals of biomechanics in tissue engineering of bone. *Tissue Eng* 2000;6(4):361-81.
16. Ethier CRS, Craig A. *Skeletal Biomechanics. Introductory Biomechanics.* Cambridge: Cambridge University Press; 2007. p. 382, 88.
17. Reves BT, Bumgardner JD, Cole JA, Yang Y, Haggard WO. Lyophilization to improve drug delivery for chitosan-calcium phosphate bone scaffold construct: a preliminary investigation. *J Biomed Mater Res B Appl Biomater* 2009;90(1):1-10.
18. Reddy GK, Enwemeka CS. A simplified method for the analysis of hydroxyproline in biological tissues. *Clin Biochem* 1996;29(3):225-9.

19. Manjubala I, Ponomarev I, Wilke I, Jandt KD. Growth of osteoblast-like cells on biomimetic apatite-coated chitosan scaffolds. *J Biomed Mater Res B Appl Biomater* 2008;84(1):7-16.
20. Rodan SB, Imai Y, Thiede MA, Wesolowski G, Thompson D, Bar-Shavit Z, et al. Characterization of a human osteosarcoma cell line (Saos-2) with osteoblastic properties. *Cancer Res* 1987;47(18):4961-6.
21. Jiang T, Nukavarapu SP, Deng M, Jabbarzadeh E, Kofron MD, Doty SB, et al. Chitosan-poly(lactide-co-glycolide) microsphere-based scaffolds for bone tissue engineering: In vitro degradation and in vivo bone regeneration studies. *Acta Biomater* 2010.
22. Jiang T, Khan Y, Nair LS, Abdel-Fattah WI, Laurencin CT. Functionalization of chitosan/poly(lactic acid-glycolic acid) sintered microsphere scaffolds via surface heparinization for bone tissue engineering. *J Biomed Mater Res A* 2009.

CHAPTER 4: SUMMARY AND CONCLUSIONS

In the United States, over 500,000 patients are in need of bone grafts for a variety of orthopedic complications including bone fractures and defects.⁵ To meet clinical demands, bone tissue engineering investigates synthetic three-dimensional matrix to provide structural support and tissue guidance.^{3, 17, 22} Scaffolds constructed from biomaterials must have suitable biomechanical properties and 3D macro- and micro-structure to be physiologically functional and support tissue infiltration and growth.^{1, 3} An ideal scaffold should elicit appropriate host responses, degrade at a rate similar to that of bone regeneration, maintain mechanical integrity, have interconnected pores for nutrient and waste exchange, promote bone cell attachment and proliferation, and facilitate bone formation.^{1, 3-5, 31, 32} Current bone scaffolds constructed from polymers, ceramics, and composites have not met the challenge with their low mechanical properties, biodegradability, and degradation rates.^{1, 4, 24} The primary objective of this research was to fabricate a composite chitosan-calcium phosphate scaffold based on air-dried and freeze-dried microspheres possessing essential design criteria including high porosity with interconnected pores for bone matrix and blood vessel ingrowth, compressive strength for load bearing, and surface chemistry promoting bone tissue growth and organization as an ideal bone graft substitute.

The composition of chitosan with nanoparticle calcium phosphate mimics the inorganic and organic composition of bone which is a synergistic pairing of a natural, biodegradable, and biocompatible polymer with a biomimetic, biomechanical, and osteoconductive bone mineral calcium phosphate.^{1, 4, 5, 17, 32} Chitosan is polysaccharide consisting of glucosamine and *N*-acetyl glucosamine with free amino and hydroxyl side

chains for protein affinity.³² Calcium phosphate is a major mineral component of bone with the innate capacity to conduct bone cell attachment, proliferation, and mineralization.¹⁶ Chitosan is the organic matrix that can uniformly encapsulate calcium phosphate nanoparticles for a functional composite bone scaffold material.^{45, 50}

A co-precipitation method was utilized to produce microsphere composite of chitosan and a bioceramic calcium phosphate.^{45, 50} Scaffolds consisting of air-dried (AD) and freeze-dried (FD) microspheres or entirely of all air-dried microspheres were compared for mechanical and degradation properties, and ability to support bone cell growth and matrix production *in vitro*. The AD and FD microspheres were arranged to mimic the cross section of long bone. The AD scaffolds were constructed entirely of AD microspheres while the FDAD combination scaffolds were solid AD microspheres lining the outer shell and the microporous FD microspheres filling the interior shell.

The surface topography and microsphere density of FD microspheres was textured and porous as opposed to the smooth surface and homogenous solid core of the AD microspheres. Reves et al. showed that the addition of FD microspheres increased surface area by 400% and porosity by 50%.⁵⁰ This provided an advantage for FD microspheres for uniform distribution of cells along with 30% increase in cell number per scaffold mass that led to the 81% greater production of total collagen per scaffold mass. However, the incorporation of the FD microspheres to the interior of the scaffold decreased the mechanical strength by 60%. Even though compressive strength was weakened, the addition of FD microspheres that are microporous with textured surface can enhance bone matrix and cell attachment. Furthermore, AD and FD microspheres can

be molded into a variety of shapes and sizes fit for non-load-bearing orthopedic applications such as craniofacial defect repair.

CHAPTER 5: FUTURE WORKS AND ALTERNATIVES

The results of the study showed potential bone scaffold characteristics for the composite chitosan calcium phosphate microsphere based scaffolds. However, there were issues that need thorough follow-up assessments before the scaffolds can be clinically applicable. First, the matrix deposition and mineralization were minimally visible under the scanning electron microscope. A repeat of the mineralization can be conducted to obtain better measurements of matrix production and mineralization by determining levels of osteocalcin, hydroxyproline, and calcium. In a previous study with similar AD scaffolds, cells seeded on the scaffolds had a growth prior to mineralization in a rotary bioreactor and the scaffolds showed bone matrix deposition occurred at day 14. The dynamic flow of the medium promoted efficient nutrient and waste exchange and induced shear stress on the cells as mechanical stimulation. By using the rotary bioreactor in a follow-up study, sufficient medium diffusion is provided for the entirety of the scaffold.

The second issue to resolve is the slow degradation of the scaffolds. The rate of scaffold degradation should be equivalent to the rate of bone formation to promote bone tissue ingrowth and consequently compensate for the loss in mechanical integrity to prevent scaffold collapse. This can be accomplished by using chitosan with different DDAs to produce the microspheres, incorporating a higher concentration of calcium phosphate nanoparticles, and using different solvent acids to dissolve the chitosan.^{32, 52}

To better understand the architectural properties of the scaffolds, a thorough characterization of scaffold macro- and micro-porosity (focusing on FD microspheres) is necessary. Pore size, interconnected porosity, surface area, and surface topography are influential in bone cell proliferation, communication, growth, and attachment,

respectively. Even though Reves et al. characterized lyophilized composite chitosan calcium phosphate scaffolds, the drying and scaffold construction techniques were different which can render different surface physico-chemistry.⁵⁰ These results can be utilized to optimize the functional potential of the AD and FD microspheres and its arrangement to mimic the organization of other bones in the body.

A major concern for bone scaffold functionality is osteoinductivity, the induction of mesenchymal stem cell (MSC) differentiation into specialized bone cells to regenerate bone. Osteoinduction can be incorporated into the scaffold by integrating growth factors, cytokines, and molecular agents that induce MCS differentiation. Bone morphogenic proteins, vascular endothelial growth factors, and platelet-derived growth factors are common factors that provoke morphogenesis of bone cells, angiogenesis vascular endothelial cells, and recruitment of inflammatory and fibroblasts, respectively. The inherent microporosity of FD microspheres having high absorption potential and protein affinity of amino acid side chains on chitosan confer advantages for growth factors and cytokine absorption.

Finally, the issue of scaffold functionality with *in vivo* models is crucial to obtain in order for the scaffolds to be used as a clinical alternative to auto- and allo-grafts. Common models are rat calvarial and rabbit radial critical size defect. Since rat calvarial and rabbit radial bone are small, scaffold composition is limited to AD or FD microspheres alone. Furthermore, scaffolds can be also loaded with growth factors to examine absorption capabilities and elution efficacy within the *in vivo* model.

References

1. BarrÈre FM, T.A.;de Groot, K.;van Blitterswijk, C.A. Advanced biomaterials for skeletal tissue regeneration: Instructive and smart functions. *Materials Science and Engineering: R: Reports* 2008;59(1-6):38-71.
2. Ethier CRS, Craig A. *Skeletal Biomechanics. Introductory Biomechanics.* Cambridge: Cambridge University Press; 2007. p. 382, 88.
3. Karande TS, Ong JL, Agrawal CM. Diffusion in musculoskeletal tissue engineering scaffolds: design issues related to porosity, permeability, architecture, and nutrient mixing. *Ann Biomed Eng* 2004;32(12):1728-43.
4. Burchardt H. The biology of bone graft repair. *Clin Orthop Relat Res* 1983(174):28-42.
5. Giannoudis PV, Dinopoulos H, Tsiridis E. Bone substitutes: an update. *Injury* 2005;36 Suppl 3:S20-7.
6. Schindeler A, McDonald MM, Bokko P, Little DG. Bone remodeling during fracture repair: The cellular picture. *Semin Cell Dev Biol* 2008;19(5):459-66.
7. Giannoudis PV, Einhorn TA, Marsh D. Fracture healing: the diamond concept. *Injury* 2007;38 Suppl 4:S3-6.
8. Wraighte PJ, Scammell BE. Principles of Fracture Healing. *General Principles of Orthopedic Surgery* 2006;24(6):198-207.
9. Carano RA, Filvaroff EH. Angiogenesis and bone repair. *Drug Discov Today* 2003;8(21):980-9.
10. Deschaseaux F, Sensebe L, Heymann D. Mechanisms of bone repair and regeneration. *Trends Mol Med* 2009;15(9):417-29.

11. Keramaris NC, Calori GM, Nikolaou VS, Schemitsch EH, Giannoudis PV. Fracture vascularity and bone healing: a systematic review of the role of VEGF. *Injury* 2008;39 Suppl 2:S45-57.
12. Soucacos PN, Johnson EO, Babis G. An update on recent advances in bone regeneration. *Injury* 2008;39 Suppl 2:S1-4.
13. Tzioupis C, Giannoudis PV. Prevalence of long-bone non-unions. *Injury* 2007;38 Suppl 2:S3-9.
14. Koo DA, D.; Copeland, T.; Hall, P. Incidence and Costs to Medicare of Fractures Among Medicare Beneficiaries Aged ≥ 65 Years — United States, July 1991–June 1992: Centers for Disease Control and Prevention; 1996.
15. Lewandrowski KU, Gresser JD, Wise DL, Trantol DJ. Bioresorbable bone graft substitutes of different osteoconductivities: a histologic evaluation of osteointegration of poly(propylene glycol-co-fumaric acid)-based cement implants in rats. *Biomaterials* 2000;21(8):757-64.
16. Khan Y, Yaszemski MJ, Mikos AG, Laurencin CT. Tissue engineering of bone: material and matrix considerations. *J Bone Joint Surg Am* 2008;90 Suppl 1:36-42.
17. Khan SN, Cammisa FP, Jr., Sandhu HS, Diwan AD, Girardi FP, Lane JM. The biology of bone grafting. *J Am Acad Orthop Surg* 2005;13(1):77-86.
18. Younger EM, Chapman MW. Morbidity at bone graft donor sites. *J Orthop Trauma* 1989;3(3):192-5.
19. Bostman O, Pihlajamaki H. Clinical biocompatibility of biodegradable orthopaedic implants for internal fixation: a review. *Biomaterials* 2000;21(24):2615-21.

20. Hofmann A, Konrad L, Hessmann MH, Kuchle R, Korner J, Rompe JD, et al. The influence of bone allograft processing on osteoblast attachment and function. *J Orthop Res* 2005;23(4):846-54.
21. Blokhuis TJ, Lindner T. Allograft and bone morphogenetic proteins: an overview. *Injury* 2008;39 Suppl 2:S33-6.
22. Langer R, Vacanti JP. Tissue engineering. *Science* 1993;260(5110):920-6.
23. Sharma B, Elisseeff JH. Engineering structurally organized cartilage and bone tissues. *Ann Biomed Eng* 2004;32(1):148-59.
24. Dawson JJ, Oreffo RO. Bridging the regeneration gap: stem cells, biomaterials and clinical translation in bone tissue engineering. *Arch Biochem Biophys* 2008;473(2):124-31.
25. Gomi K, Lowenberg B, Shapiro G, Davies JE. Resorption of sintered synthetic hydroxyapatite by osteoclasts in vitro. *Biomaterials* 1993;14(2):91-6.
26. Lu X, Leng Y. Quantitative analysis of osteoblast behavior on microgrooved hydroxyapatite and titanium substrata. *J Biomed Mater Res A* 2003;66(3):677-87.
27. Tsiridis E, Upadhyay N, Giannoudis P. Molecular aspects of fracture healing: which are the important molecules? *Injury* 2007;38 Suppl 1:S11-25.
28. Adachi T, Osako Y, Tanaka M, Hojo M, Hollister SJ. Framework for optimal design of porous scaffold microstructure by computational simulation of bone regeneration. *Biomaterials* 2006;27(21):3964-72.
29. Alsberg E, Kong HJ, Hirano Y, Smith MK, Albeiruti A, Mooney DJ. Regulating bone formation via controlled scaffold degradation. *J Dent Res* 2003;82(11):903-8.

30. Cullen DM, Smith RT, Akhter MP. Time course for bone formation with long-term external mechanical loading. *J Appl Physiol* 2000;88(6):1943-8.
31. Athanasiou KA, Zhu C, Lanctot DR, Agrawal CM, Wang X. Fundamentals of biomechanics in tissue engineering of bone. *Tissue Eng* 2000;6(4):361-81.
32. Di Martino A, Sittinger M, Risbud MV. Chitosan: a versatile biopolymer for orthopaedic tissue-engineering. *Biomaterials* 2005;26(30):5983-90.
33. Bolander ME. Regulation of fracture repair by growth factors. *Proc Soc Exp Biol Med* 1992;200(2):165-70.
34. Einhorn TA, Majeska RJ, Rush EB, Levine PM, Horowitz MC. The expression of cytokine activity by fracture callus. *J Bone Miner Res* 1995;10(8):1272-81.
35. Jiang T, Khan Y, Nair LS, Abdel-Fattah WI, Laurencin CT. Functionalization of chitosan/poly(lactic acid-glycolic acid) sintered microsphere scaffolds via surface heparinization for bone tissue engineering. *J Biomed Mater Res A* 2009.
36. Yilgor P, Tuzlakoglu K, Reis RL, Hasirci N, Hasirci V. Incorporation of a sequential BMP-2/BMP-7 delivery system into chitosan-based scaffolds for bone tissue engineering. *Biomaterials* 2009;30(21):3551-9.
37. Zhang Y, Shi B, Li C, Wang Y, Chen Y, Zhang W, et al. The synergetic bone-forming effects of combinations of growth factors expressed by adenovirus vectors on chitosan/collagen scaffolds. *J Control Release* 2009;136(3):172-8.
38. Porter JR, Ruckh TT, Papat KC. Bone tissue engineering: a review in bone biomimetics and drug delivery strategies. *Biotechnol Prog* 2009;25(6):1539-60.

39. Xu HH, Quinn JB, Takagi S, Chow LC. Synergistic reinforcement of in situ hardening calcium phosphate composite scaffold for bone tissue engineering. *Biomaterials* 2004;25(6):1029-37.
40. Guo H, Su J, Wei J, Kong H, Liu C. Biocompatibility and osteogenicity of degradable Ca-deficient hydroxyapatite scaffolds from calcium phosphate cement for bone tissue engineering. *Acta Biomater* 2009;5(1):268-78.
41. Kim SS, Sun Park M, Jeon O, Yong Choi C, Kim BS. Poly(lactide-co-glycolide)/hydroxyapatite composite scaffolds for bone tissue engineering. *Biomaterials* 2006;27(8):1399-409.
42. Li LH, Kommareddy KP, Pilz C, Zhou CR, Fratzl P, Manjubala I. In vitro bioactivity of bioresorbable porous polymeric scaffolds incorporating hydroxyapatite microspheres. *Acta Biomater* 2010;6(7):2525-31.
43. Wu L, Ding J. In vitro degradation of three-dimensional porous poly(D,L-lactide-co-glycolide) scaffolds for tissue engineering. *Biomaterials* 2004;25(27):5821-30.
44. Zhang P, Hong Z, Yu T, Chen X, Jing X. In vivo mineralization and osteogenesis of nanocomposite scaffold of poly(lactide-co-glycolide) and hydroxyapatite surface-grafted with poly(L-lactide). *Biomaterials* 2009;30(1):58-70.
45. Chesnutt BM, Viano AM, Yuan Y, Yang Y, Guda T, Appleford MR, et al. Design and characterization of a novel chitosan/nanocrystalline calcium phosphate composite scaffold for bone regeneration. *J Biomed Mater Res A* 2009;88(2):491-502.

46. Wu YC, Shaw SY, Lin HR, Lee TM, Yang CY. Bone tissue engineering evaluation based on rat calvaria stromal cells cultured on modified PLGA scaffolds. *Biomaterials* 2006;27(6):896-904.
47. Khor E, Lim LY. Implantable applications of chitin and chitosan. *Biomaterials* 2003;24(13):2339-49.
48. Jiang T, Abdel-Fattah WI, Laurencin CT. In vitro evaluation of chitosan/poly(lactic acid-glycolic acid) sintered microsphere scaffolds for bone tissue engineering. *Biomaterials* 2006;27(28):4894-903.
49. Thein-Han WW, Misra RD. Biomimetic chitosan-nanohydroxyapatite composite scaffolds for bone tissue engineering. *Acta Biomater* 2009;5(4):1182-97.
50. Reves BT, Bumgardner JD, Cole JA, Yang Y, Haggard WO. Lyophilization to improve drug delivery for chitosan-calcium phosphate bone scaffold construct: a preliminary investigation. *J Biomed Mater Res B Appl Biomater* 2009;90(1):1-10.
51. Xu HH, Takagi S, Quinn JB, Chow LC. Fast-setting calcium phosphate scaffolds with tailored macropore formation rates for bone regeneration. *J Biomed Mater Res A* 2004;68(4):725-34.
52. Ren D, Yi H, Wang W, Ma X. The enzymatic degradation and swelling properties of chitosan matrices with different degrees of N-acetylation. *Carbohydr Res* 2005;340(15):2403-10.
53. Shi C, Zhu Y, Ran X, Wang M, Su Y, Cheng T. Therapeutic potential of chitosan and its derivatives in regenerative medicine. *J Surg Res* 2006;133(2):185-92.

54. Lee JY, Nam SH, Im SY, Park YJ, Lee YM, Seol YJ, et al. Enhanced bone formation by controlled growth factor delivery from chitosan-based biomaterials. *J Control Release* 2002;78(1-3):187-97.
55. Xu HH, Simon CG, Jr. Fast setting calcium phosphate-chitosan scaffold: mechanical properties and biocompatibility. *Biomaterials* 2005;26(12):1337-48.
56. Jiang T, Nukavarapu SP, Deng M, Jabbarzadeh E, Kofron MD, Doty SB, et al. Chitosan-poly(lactide-co-glycolide) microsphere-based scaffolds for bone tissue engineering: In vitro degradation and in vivo bone regeneration studies. *Acta Biomater* 2010.

Appendix 1

Apparent Density of AD and FDAD scaffolds

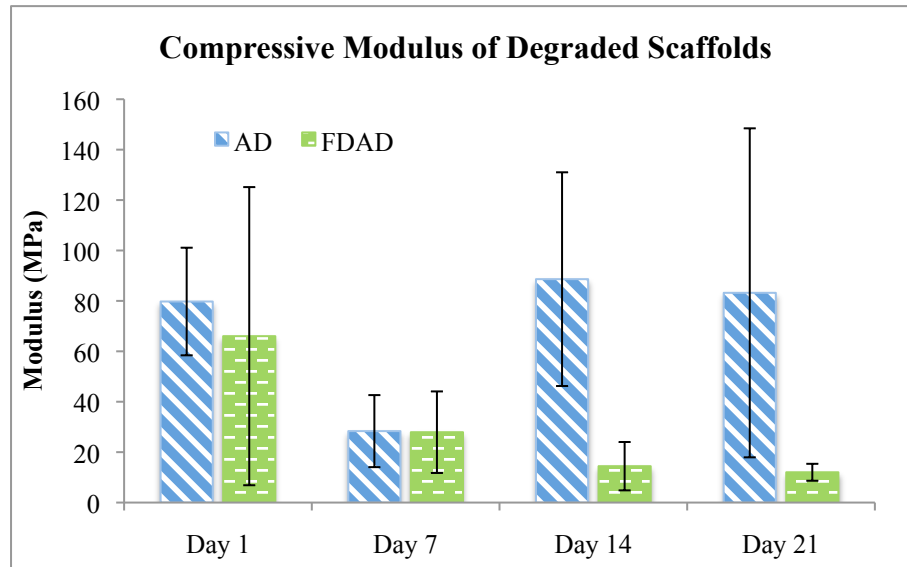
BULK VOLUME (CM ³)															
AD	Outer diameter (m)	Outer Height (m)	inner diameter	height	AD	Outer diameter (m)	Outer Height (m)	inner diameter	height	AD	Outer diameter (m)	Outer Height (m)	inner diameter	height	
1	12.58	6.10	3.50	6.10	6.10	1	12.65	6.23	3.56	6.23	1	12.53	5.70	3.62	5.70
2	12.55	6.13	3.59	6.13	6.28	2	12.68	6.28	3.84	6.28	2	12.60	5.65	3.19	5.65
3	12.39	6.10	3.53	6.10	5.79	3	12.66	5.79	3.70	5.79	3	12.46	5.80	3.32	5.80
4	12.30	6.06	3.66	6.06	5.92	4	12.62	5.92	3.62	5.92	4	12.59	5.82	3.57	5.82
average	12.46	6.10	3.57	6.10	6.06	average	12.65	6.06	3.68	6.06	average	12.55	5.74	3.43	5.74
radius	6.23	6.10	1.79	6.10	1.84	radius	6.33	1.84	1.84	1.84	radius	6.27	1.71	1.71	1.71
cm	0.62	0.61	0.18	0.61	0.61	cm	0.63	0.61	0.18	0.61	cm	0.63	0.57	0.17	0.57
volume (cm ³)	0.74	0.74	0.06	0.74	0.76	volume (cm ³)	0.76	0.76	0.06	0.76	volume (cm ³)	0.71	0.71	0.05	0.71
total volume	0.682	0.682	0.06	0.682	0.697	total volume	0.697	0.697	0.06	0.697	total volume	0.657	0.657	0.05	0.657
FD/AD	Outer diameter (m)	Outer Height (m)	inner diameter	height	FD/AD	Outer diameter (m)	Outer Height (m)	inner diameter	height	FD/AD	Outer diameter (m)	Outer Height (m)	inner diameter	height	
1	11.49	6.62	2.60	6.62	5.90	1	11.89	5.90	3.34	5.90	1	12.07	6.52	2.27	6.52
2	11.62	6.29	3.32	6.29	6.07	2	11.93	6.07	3.22	6.07	2	11.98	6.81	2.69	6.81
3	11.58	6.37	2.81	6.37	5.76	3	11.88	5.76	3.06	5.76	3	11.95	6.53	3.33	6.53
4	11.57	6.30	2.86	6.30	5.92	4	12.03	5.92	3.08	5.92	4	11.96	6.66	3.58	6.66
average	11.57	6.40	2.90	6.40	5.91	average	11.93	5.91	3.18	5.91	average	11.99	6.63	2.97	6.63
radius	5.78	6.40	1.45	6.40	1.59	radius	5.97	1.59	1.59	1.59	radius	6.00	1.48	1.48	1.48
cm	0.58	0.64	0.14	0.64	0.59	cm	0.60	0.59	0.16	0.59	cm	0.60	0.66	0.15	0.66
volume (cm ³)	0.67	0.67	0.04	0.67	0.66	volume (cm ³)	0.66	0.66	0.05	0.66	volume (cm ³)	0.73	0.73	0.05	0.73
total volume	0.630	0.630	0.04	0.630	0.614	total volume	0.614	0.614	0.05	0.614	total volume	0.703	0.703	0.05	0.703
MASS (g)	AD	FD/AD				DISPLACEMENT (CM ³)	AD	FD/AD							
1	0.6048	0.3644				1	3.4	0.4			1	7	7.5	0.4	
2	0.6001	0.3524				2	3.4	0.4			2	7.5	7.9	0.5	
3	0.6014	0.3789				3	3.8	4.3			3	7.9	8.4	0.5	
4	0.6038	0.3524				4	5.2	5.7			4	9	9.3	0.3	
First Measurement						Particle Dens AD		FD/AD			Particle Dens AD		FD/AD		
Bulk Density AD	1	0.887	0.579			1	12.5	0.4			1	12.10	0.911		
2	0.861	0.574				2	12.9	0.5			2	1500	1.175		
3	0.916	0.539				3	13.4	0.5			3	1203	0.947		
4	0.914	0.562				4	13.9	0.5			4	1208	0.881		
Particle Dens AD		FD/AD				Apparent De AD		FD/AD			Apparent De AD		FD/AD		
1	1.512	0.729				1	41.34%	20.59%			1	26.67%	36.47%		
2	1.500	0.881				2	42.60%	34.89%			2	42.60%	51.17%		
3	1.203	0.758				3	23.88%	28.85%			3	23.88%	43.08%		
4	1.208	1.175				4	24.28%	52.16%			4	24.28%	56.21%		
Apparent De AD		FD/AD													

Second Measurement using the same Scaffolds

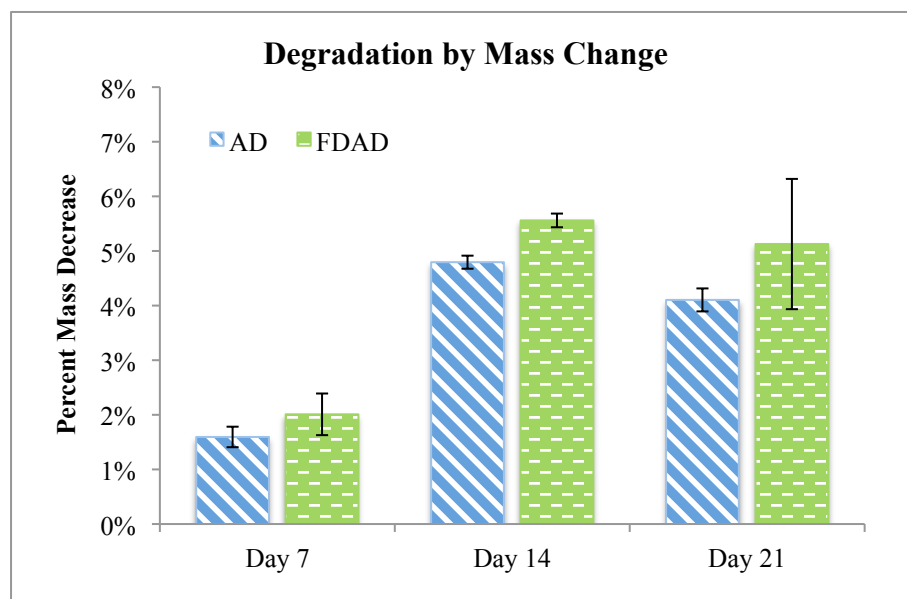
AD	Outer diameter (m)	Outer Height (m)	inner diameter	height	AD	Outer diameter (m)	Outer Height (m)	inner diameter	height
1	12.65	6.23	3.56	6.23	1	12.53	5.70	3.62	5.70
2	12.68	6.28	3.84	6.28	2	12.60	5.65	3.19	5.65
3	12.66	5.79	3.70	5.79	3	12.46	5.80	3.32	5.80
4	12.62	5.92	3.62	5.92	4	12.59	5.82	3.57	5.82

Appendix 2

Degradation study on AD and FDAD scaffolds conducted in December 2009



There is a significant difference between the scaffold types ($p=0.005$) but no differences over time.



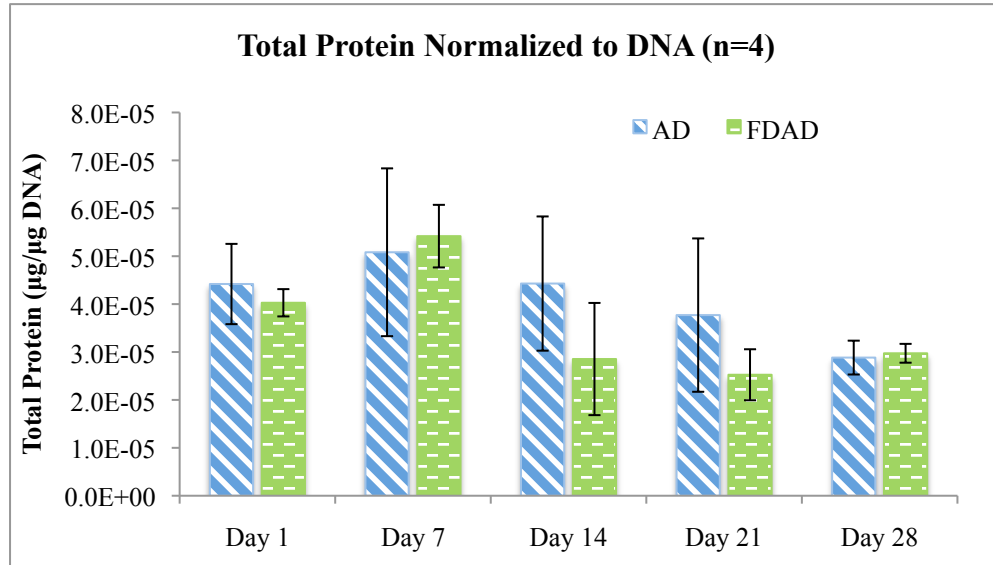
There is significant difference between the two scaffold types ($p<0.001$) and over time ($p=0.002$).

Appendix 3

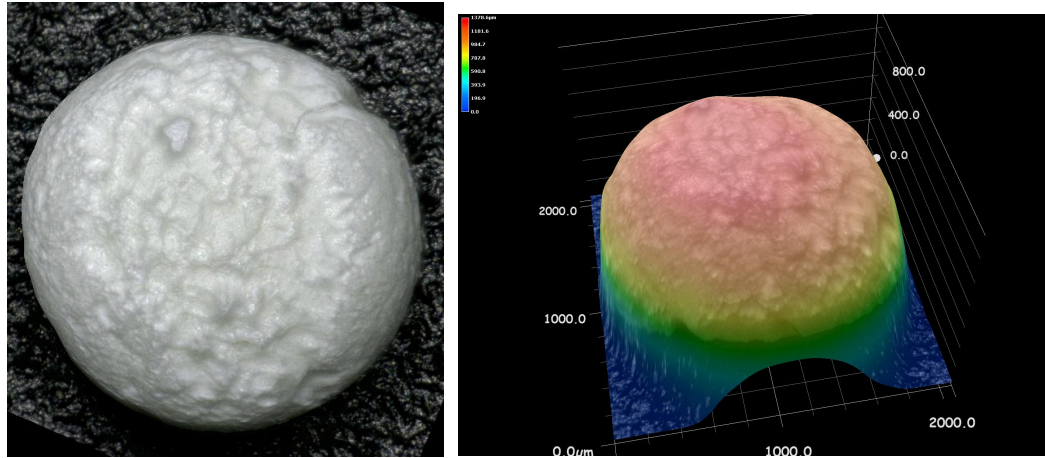
Modulus of AD Scaffolds Hydrated for 4hrs in Water or PBS Calculated from BlueHill	
	Modulus (MPa)
Scaffold A - Water	95.48
Scaffold B - Water	76.02
Scaffold A - PBS	87.87
Scaffold B - PBS	97.79

Appendix 4

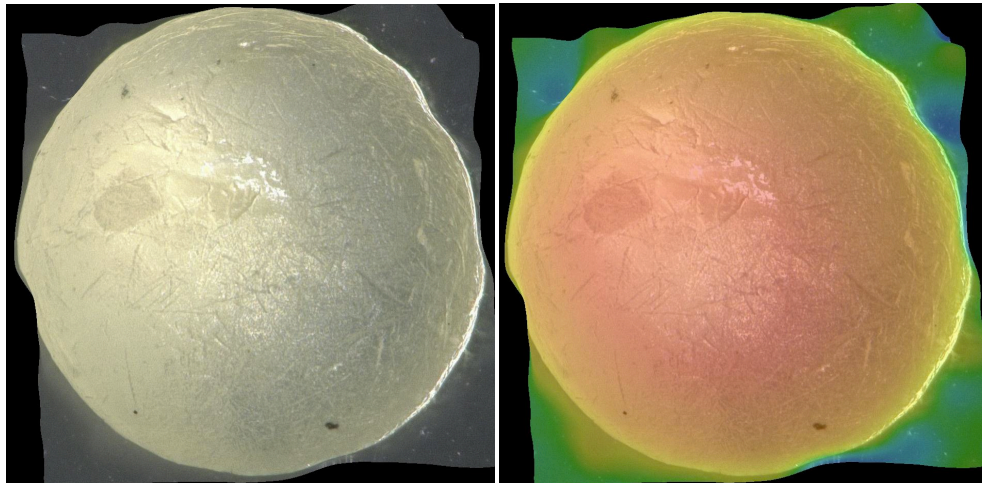
AD vs FDAD mineralization measurement of total protein



Appendix 5



FD microsphere taken from Keyence VHX-1000 digital microscope.



AD microsphere. Top view.

Appendix 6

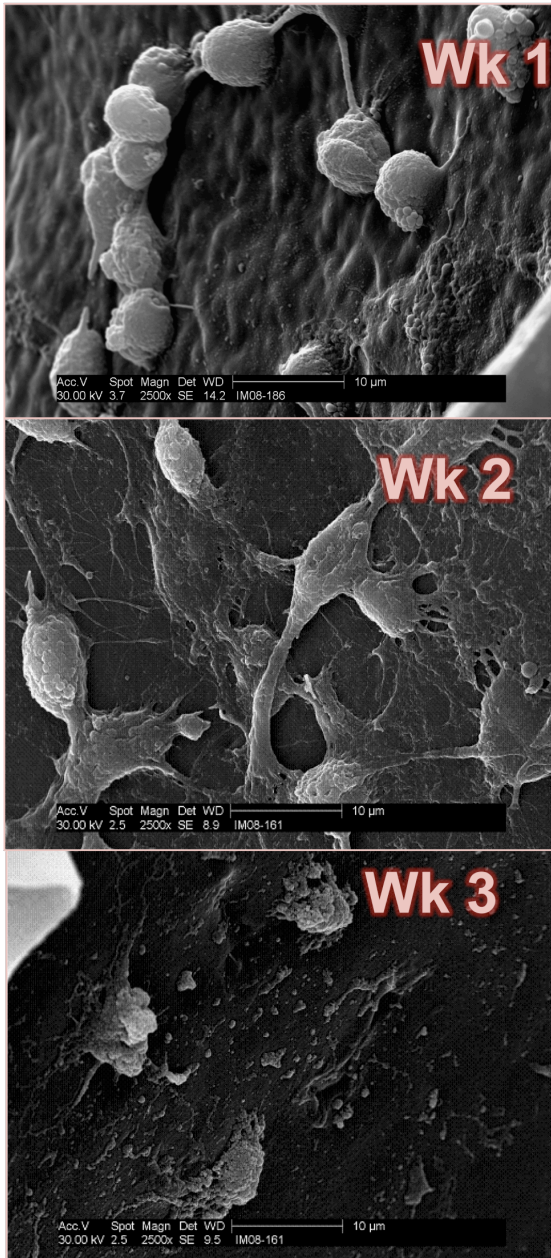
Rotary bioreactor



Appendix 7

Comparison of culture conditions with all AD scaffolds conducted 2008

Static @ 2500x



Rotary @ 2500x

